Parameterization of invariant manifolds for periodic orbits(I): efficient numerics via the Floquet normal form

Roberto Castelli * Jean-Philippe Lessard† J.D. Mireles James ‡

May 27, 2014

Abstract

We present an efficient numerical method for computing Fourier-Taylor expansions of (un)stable manifolds associated with hyperbolic periodic orbits. Three features of the method are that (1) we obtain accurate representation of the invariant manifold as well as the dynamics on the manifold, (2) it admits natural a-posteriori error analysis, and (3) it does not require numerically integrating the vector field. Our approach is based on the Parameterization Method for invariant manifolds, and studies a certain partial differential equation which characterizes a chart map of the manifold. The method requires only that some mild non-resonance conditions hold. The novelty of the present work is that we exploit the Floquet normal form in order to efficiently compute the Fourier-Taylor expansion. A number of example computations are given including manifolds in phase space dimension as high as ten and manifolds which are two and three dimensional. We also discuss computations of cycle-to-cycle connecting orbits which exploit these manifolds.

1 Introduction

Equilibria and periodic orbits of nonlinear systems are building blocks for understanding global dynamics. The basins of attraction, repulsion, and stable/unstable manifolds associated with these building blocks provide information about how phase space fits together. The equilibria and periodic orbits together with their stable/unstable manifolds form an invariant skeleton which governs transitions from one region of phase space to another, describes where mixing and stagnation occur, and in some cases establishes the existence and whereabouts of chaotic motions. Given a particular nonlinear systems it is often difficult to represent periodic orbits and their invariant manifolds in closed form, hence substantial effort has gone into developing numerical methods for approximating these objects.

In this paper we present an efficient scheme for computing numerical approximations of local stable/unstable manifolds associated with hyperbolic periodic orbits of differential equations. The inputs to the method are a Fourier approximation for the periodic orbit *in addition to a Fourier approximation of the Floquet normal form*. The method developed here applies to hyperbolic periodic orbits under mild non-resonance assumptions.

*BCAM - Basque Center for Applied Mathematics, Alameda Mazarredo 14, 48009, Bilbao, Basque Country, SPAIN. Email: rcastelli@bcamath.org.

†Université Laval, Département de Mathématiques et de Statistique, Pavillon Alexandre-Vachon, 1045 avenue de la Médecine, Québec, QC, G1V 0A6, CANADA. Email: jean-philippe.lessard@mat.ulaval.ca.

‡Rutgers University, Department of Mathematics,110 Frelinghuysen Rd, Piscataway, NJ 08854, USA. jmireles@math.rutgers.edu .

In order to illustrate some results which are obtained using our method we include Figures 1 and 2 in the present introductory section. The figures show the local stable and unstable invariant manifolds associated with a saddle periodic orbit on the global chaotic attractor of the Lorenz equations at the classical parameter values.

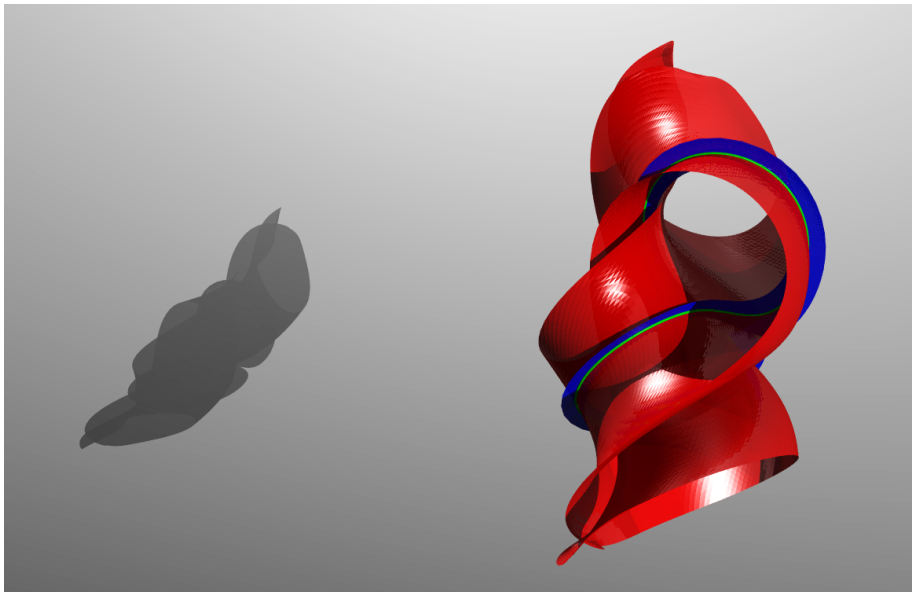

Figure 1: Local stable (red) and unstable (blue) manifolds associated with a hyperbolic periodic orbit Γ (green) in the Lorenz attractor. This computation is carried out for the classical parameter values $\rho = 28$, $s = 10$ and $\beta = 8/3$. The figure illustrates the images of parameterizations truncated to Taylor order $N = 25$ and $K = 66$ Fourier modes. No integration is performed in order to globalize the manifold. The stable manifold is not the graph of a function over the stable linear bundle of Γ. This highlights an important feature of the Parameterization Method which is that it can follow folds in the manifolds. The figure also illustrates the stretching and folding of the phase space near Γ.

Our method is based on the *Parametrization Method* introduced in [45, 46, 47], and the idea is to study an *invariance equation* describing the invariant manifold. One plugs a certain formal series into the invariance equation and solves the problem via a power matching scheme. As we will show, this procedure leads to a sequence of linear ordinary differential equations with periodic coefficients which then needs to be solved recursively.

From the theoretical point of view the existence of solutions for these equations is well understood provided certain resonance conditions are satisfied. Abstract convergence of the Fourier-Taylor series is discussed in [47, 71]. From a numerical point of view these equations can be solved to any desired finite order, resulting in an expansion which approximates the local manifold as well as we wish near the periodic orbit. In order to implement this scheme we have to numerically solve the recursive system efficiently. We would like to have indicators which describe how good our approximate solution is near the periodic orbit.

In the present work we exploit the fact that an invertible change of coordinates, which we define in terms of the Floquet normal form, reduces each of the differential equations in the recursive scheme to constant coefficient. The transformed equations are solved in Fourier space, resulting in algebraic recurrence relations. Inverting the coordinate transformation

gives us the desired coefficients for the parameterization. We also discuss a reliable and easy to implement a-posteriori error indicator which allows us to estimate the size of the domain on which our numerical solution provides a good approximation.

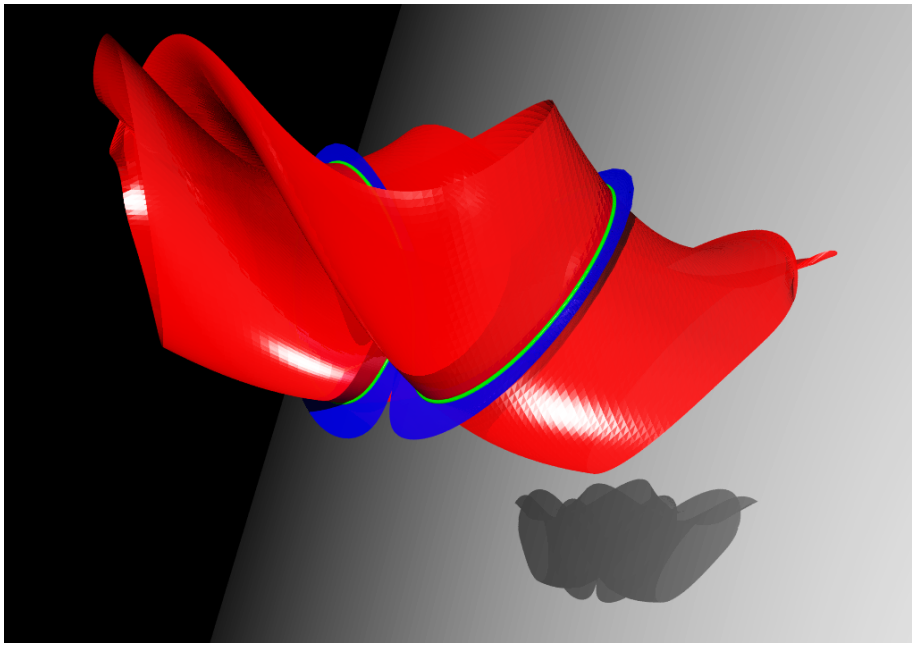

Figure 2: Local stable (red) and unstable (blue) manifolds of a hyperbolic periodic orbit Γ (green) in the Lorenz attractor at the classical values $\rho = 28$, $s = 10$ and $\beta = 8/3$. This figure illustrates that the Parameterization Method provides expansions for the local invariant manifolds which are valid in rather large regions about Γ, and which expose nonlinear features of the manifolds. For example the local stable manifold shown here is roughly as wide as the global attractor itself. Both manifolds are parameterized by Fourier-Taylor expansions and no numerical integration has been employed in order to globalize the results.

Remark 1.1 (Computation of the periodic orbit and its Floquet normal form). The periodic orbit and its Floquet normal form are computed using Fourier spectral methods. The Fourier expansions of the orbit and of the normal form are taken as the inputs for the invariant manifold computations. The use of spectral methods to study periodic solutions of differential equations has a rich history and we make no attempt to review the literature on the subject. The interested reader can consult [63, 48, 58, 70, 71, 80]. The approach used in [71, 80] is especially relevant to the present work. In fact [80] provides rigorous bounds associated with spectral Fourier approximations of the Floquet normal form, which could be used to provide rigorous bounds on the initial data for the present approach.

Remark 1.2 (Validated numerics). Combining the work of [80] with the present work will lead to methods for obtaining rigorous bounds on the truncation error associated with our parameterization. See also the discussion in Section 5 of [47]. Once rigorous a-posteriori bounds on the Fourier-Taylor expansions of the local manifolds are known it is possible to extend the methods of [62, 59, 60] to obtain computer assisted proof of transverse cycle-to-cycle and cycle-to-point connections for differential equations. Computer assisted validation for stable/unstable manifolds for periodic orbits is the topic of paper II.

The remainder of the paper is organized as follows. In Section 1.1 we provide some brief remarks on the literature. Section 2 comprises the mathematical core of the paper. Here we review the Floquet theory as well as the Parameterization Method. We derive the recursive system of differential equations for the Taylor coefficients of the manifold and solve the system via the Floquet normal form. Finally we discuss an a-posteriori error indicator for the method. Section 3 deals with numerical computations. We begin with a detailed discussion of the computations illustrated in Figures 1 and 2. We also discuss the computation of some three dimensional stable manifolds for periodic orbits for three dimensional vector fields (these manifolds provide trapping regions, and generalize to three dimensions the work of [71, 72]). Finally we discuss the computation of some invariant manifolds for a ten dimensional differential equation which arises as a truncation of the Kuramoto-Sivashinsky PDE. The final section of the paper is Section 4 and we present some examples where the parameterized manifolds are used to compute homoclinic connecting orbits of periodic orbits via the method of projected boundaries. We look at some examples for the Lorenz system and also for a ten-dimensional Galerkin projection of the Kuramoto-Sivashinsky PDE.

1.1 Related work

The literature on numerical computation of invariant objects for dynamical systems is vast and we attempt only a brief overview. Our primary objective is to direct the interested reader to more complete sources of information.

The central role to be played by invariant manifolds in the qualitative theory of dynamical systems is already anticipated in the work of Poincaré. (See for example the historical discussion of this work found in Appendix B of [47]). By the mid 20-th Century results such as [52] made precise the fact that intersections of stable and unstable manifolds give rise to complicated dynamics. The advent of the computer as a tool for studying the dynamics of nonlinear systems led to much interest in numerical methods for computing invariant manifolds and their intersection, and by the mid 1980s there were already a number of researchers using the computer to study the intersections which Poincaré remarked were difficult to draw. See the discussion in [37, 6, 7] and again the historical overview in [47].

Interest in the intersection of stable and unstable manifolds for applications has led to a great deal of work on numerical methods for globalizing local invariant manifolds. We refer the reader to the works of [25, 23, 22, 21, 20, 19, 42, 43] as well as to the review article [18]. The paper [24] treats the globalization of non-orientable stable/unstable manifolds of periodic orbits in differential equations, a subject which is also treated using the techniques of the present work. We also refer to [23, 26, 27] for studies which investigate global information about a dynamical system by studying the embedding of numerically globalized manifolds.

The region of phase space near an equilibria or a periodic orbit can also be studied via the computation of normal forms, and by evaluating these normal forms on the stable or unstable subspaces one obtains numerical methods for computing stable and unstable manifolds. These computations can be made mathematically rigorous and play a critical role in the computer assisted proof of the existence of the Lorenz attractor [77, 78, 79]. See also [86] for an application of mathematically rigorous computation for invariant manifolds in celestial mechanics based on normal forms. Normal forms are also useful for computing invariant tori, and are used in the numerical study of many problems coming from celestial mechanics [28, 5, 38, 84, 85].

The Parameterization Method is a general functional analytic framework for studying invariant manifolds of nonlinear dynamical systems. The method was initially developed for studying stable/unstable manifolds associated with non-resonant fixed points of maps and equilibria of vector fields [45, 46, 47]. Chart maps computed using the parameterization

have the additional property that they conjugate the dynamics on the invariant manifold to the dynamics of some well understood model system. Hence the method provides insight into the dynamics on the manifold as well as information about the embedding.

The Parameterization Method has been extended to study invariant circles and invariant tori for diffeomorphisms and differential equations, and is used to study stable/unstable manifolds of invariant circles [66, 67, 73, 74, 75]. More recently it has been extended to simultaneously compute invariant circles together with unknown conjugating dynamics [68, 69]. The Parameterization Method is also used in order to study some invariant manifolds associated with fixed points having some stable and some unstable directions [57].

Numerical methods for computing invariant manifolds based on the Parameterization Method can be found in a number of works including [55, 56, 71, 72, 42, 43, 82], along with the present work. A useful feature is that they admit natural a-posteriori error indicators. This notion can be used to obtain mathematically rigorous error bounds on the numerical approximation of the invariant manifolds by computer assisted analysis [62, 59, 60].

Another important application of the Parameterization Method is the development of KAM results which do not rely on the construction of action angle variables [65, 64]. There is also work which uses this method to devise KAM schemes for volume preserving diffeomorphisms [83, 82]. The Parameterization Method has recently been used in order to develop KAM type theorems for dissipative systems [76] which are conformally symplectic.

One motivation for studying stable and unstable manifolds, as mentioned above, is the fact that their intersections give rise to orbits which connect different regions of phase space. Numerical methods for computing connecting orbits between many geometric objects are found for example in the work of [6, 7, 29, 31, 32, 34, 35, 36, 44, 49, 50]. Connecting orbits between invariant manifolds are exploited in many applications. Much work on studying transfer dynamics in celestial mechanics exploits these tools [2, 3, 4, 8, 9, 10, 11, 12, 33, 40, 41]. The study of invariant manifolds for periodic orbits also plays a role in the study of biological and chemical oscillations [15, 13, 17, 16, 71, 72]. The study of connecting orbits can be made mathematically rigorous using computer assisted proofs, and we refer to [53, 54, 62, 60, 59] for more discussion of this theme.

Remark 1.3 (Computation of a local manifold versus globalization). We remark that numerical methods based on the Parameterization Method, such as [55, 56, 71, 72] and the present work, are methods for computing accurate local representations of the stable/unstable manifolds of invariant objects. In order to understand the global dynamics of a system it is natural to try to extend the local manifold via numerical integration.

This is a notoriously delicate problem as the flow induced by the vector field will stretch the boundary of the local manifold in highly nonlinear ways. For example simply numerically integrating points on the boundary of the unstable manifold for time $T > 0$ often yields unsatisfactory results, as the tendency is for the globalized object to grow much faster in some directions than in others. The numerical methods discussed in [18] provide techniques for globalizing local representations of stable/unstable manifolds in uniform ways.

An interesting line of research is to develop numerical schemes which apply globalization methods to the high order local manifold approximations given by the Parameterization Method. The papers [42, 43] develop some techniques which show that this is a fruitful line of inquiry. The Parameterization Method can be used to obtain differential geometric information (such as curvature) about stable/unstable manifolds away form the orbit, and also provides information about inflowing/outflowing properties of the flow on the boundary of the local approximation. To the best of our knowledge no attempt has been made to develop globalization schemes which exploit this information. Globalization of local invariant manifolds is not considered further in the present work.

2 Parameterization method for invariant manifolds of periodic orbits

In this section we review the Floquet theory and as much of the Parameterization Method as is used in the remainder of the present work. We also discuss the computation of the parameterization coefficients, the definition of the a-posteriori indicator function, and the effect the properties of the Floquet normal form have on the parameterization.

2.1 Floquet normal form associated to a periodic orbit

Given a periodic orbit the first order approximation of the stable invariant manifold is given by the stable normal bundle of the periodic orbit. The normal bundle is obtained by solving the variational equation around the periodic orbit. To be more precise suppose $\gamma(t) : [0, \tau] \to \mathbb{R}^d$ is a τ-periodic solution for the system $\dot{x} = f(x)$ and τ is the minimal period. Denote by $\Gamma \stackrel{\text{def}}{=} \{\gamma(t) : t \in [0, \tau]\}$ the associated periodic orbit. The variational equation is the system obtained by linearization of the vector field around $\gamma(t)$, that is

$$\begin{cases} \dot{\Phi} = Df(\gamma(t))\Phi \\ \Phi(0) = I. \end{cases} \tag{1}$$

The solution $\Phi(\tau)$ of the above system after one period is called the *monodromy matrix* of the periodic solution $\gamma(t)$. The eigenvalues ϕ_i of $\Phi(\tau)$ are the *Floquet multipliers* of Γ, and they are the eigenvalues of the differential of the Poincaré map at the fixed point. A *Floquet exponent* of Γ is any complex number μ_i such that $\phi_i = e^{\mu_i \tau}$. The unique real number ℓ_i such that $|\phi_i| = e^{\ell_i \tau}$ is called a *Lyapunov exponent* of Γ. The periodic orbit Γ is *hyperbolic* if none of its Floquet multiplier is on the unit circle. The number of Floquet multipliers inside and outside the complex unit ball determines the dimension of the stable manifold $W^s(\Gamma)$ and the dimension of the unstable manifold $W^u(\Gamma)$. The eigenvectors associated to the Floquet multipliers determine the stable/unstable directions normal to the periodic orbit at the point $\gamma(0) = \gamma(\tau)$. Denote by E_s^0, E_u^0 the space spanned by the eigenvectors associated with the stable and unstable direction respectively. In order to have a complete bundle around the orbit, one should repeat the above procedure for any of the reparametrization $\gamma^\theta(t) \stackrel{\text{def}}{=} \gamma(t + \theta)$ yielding the monodromy matrices $\Phi^\theta(\tau)$ and the stable and unstable subspaces E_s^θ, E_u^θ in $\gamma(\theta)$. Thus one defines the normal bundles of Γ as

$$E_s = \bigcup_{\theta \in [0,\tau]} \gamma(\theta) \times E_s^\theta, \quad E_u = \bigcup_{\theta \in [0,T]} \gamma(\theta) \times E_u^\theta \, .$$

As mentioned above, the knowledge of the normal bundles is fundamental for the parametrization of the invariant manifolds but the computation of E_s and E_u is not trivial. In terms of the stable/unstable manifold the essential point is that the normal bundles are the first order jets, that is the invariant manifolds are tangent to these linear bundles.

A classical method for computing the linear bundles is described in [14]. It is known that it is enough to compute the tangent directions only once, for instance for $\theta = 0$, and use the Floquet normal form of the fundamental matrix solution of the variational system to compute the entire bundles. The *real Floquet normal form* decomposition of the solution $\Phi(t)$ of system (1), is a 2τ-periodic matrix function $Q(t)$ and a real matrix R such that

$$\Phi(t) = Q(t)e^{Rt}. \tag{2}$$

The fundamental dynamical feature of the Floquet normal form is the following: if $\{\phi_i\}_i$ denote the eigenvalues and $\{w_i\}_i$ the eigenvectors of $\Phi(\tau)$ then the eigenvector $w_i(\theta)$ associated to the eigenvalue ϕ_i of the matrix $\Phi^\theta(\tau)$ are simply given by

$$w_i(\theta) \stackrel{\text{def}}{=} Q(\theta)w_i. \tag{3}$$

With this notation, we identify $w_i(0)$ with w_i. The Floquet normal form of $\Phi(t)$ provides a complete parametrization of the stable and unstable normal bundles for Γ. The function $Q(t)$ being 2τ-periodic implies that the *dynamics* of the eigenvectors $w_i(\theta)$ around the periodic orbit Γ is also 2τ-periodic. Since the tangent bundle is clearly τ-periodic it means that $w_i(0) = \pm w_i(\tau)$. If 2τ is the minimal period of Q, then $w_i(0) = -w_i(\tau)$ and the bundle is said to have a twist. This occurs when the bundle is non-orientable. In Remark 2.3, we relate the orientability of the bundle with the eigenvalues of the matrix B arising in the complex Floquet normal form, which we now introduce.

Remark 2.1 (**Complex Floquet normal form).** The *complex Floquet normal form* decomposition of the solution $\Phi(t)$ of system (1), is a (possibly complex) τ-periodic matrix function $P(t)$ and a (possibly complex) constant matrix B such that

$$\Phi(t) = P(t)e^{Bt}. \tag{4}$$

Let R be the real matrix from the real Floquet normal form (2) and B be a (possibly complex) matrix from the complex Floquet normal form (4). The following remark shows how the eigenvalues of both R and B determine the stability of a hyperbolic periodic orbit.

Remark 2.2 (**Stability of the orbit via the Floquet normal forms).** Each eigenvalue of B is a Floquet exponent of Γ. A triple $(\mu_i, \lambda_i, \phi_i)$ consisting of an eigenvalue μ_i of B, an eigenvalue λ_i of R and a Floquet multiplier ϕ_i are related by the equations $\phi_i^2 = (e^{\mu_i \tau})^2 = e^{\lambda_i 2\tau}$. While knowledge of λ_i alone is not enough to identify the Floquet multiplier ϕ_i, each eigenvalue μ_i of B (a Floquet exponent) yields uniquely a Floquet multiplier via the relation $\phi_i = e^{\mu_i \tau}$. The matrices B and R have the same eigenvectors which are also eigenvectors of $\Phi(\tau)$ and $\Phi(2\tau)$. A Lyapunov exponent ℓ_i satisfies $\ell_i = \mathrm{Re}(\mu_i) = \mathrm{Re}(\lambda_i)$. The dimension of the stable manifold of Γ, denoted by $\dim(W^s(\Gamma))$ is determined by one of the following three equivalent numbers: (a) the number of Floquet multipliers inside the unit circle; (b) the number of Floquet exponents with negative real part; (c) the number of negative Lyapunov exponents. A similar description holds for the dimension of the unstable manifold of Γ, denoted by $\dim(W^u(\Gamma))$. Three conclusions follow from the above discussion.

- The eigenvalues of both R and B determine the stability of Γ.
- The eigenvectors of R, B, $\Phi(\tau)$ and $\Phi(2\tau)$ are the same, and they determine the linear stable and unstable bundles via the relation (3).
- The eigenvalues of B are the Floquet exponents and they determine the Floquet multipliers. This is not the case for the eigenvalues of R.

The orientability of the linear bundles is obtained by the Floquet multipliers: the sign of the real part of the Floquet multipliers tells us wether the orientation of the associated eigenvector is flipped by the Poincaré map or not. If the real part is positive then the associated eigenvector is not flipped while if the real part is negative then the eigenvector is flipped. If the orientation of the eigenvector is flipped then the linear bundle is a Mobius strip. The presence of complex conjugate multipliers implies that the dynamics in the linear bundle is rotational.

The last conclusion of Remark 2.2 states that the Floquet multipliers are determined by the eigenvalues of B (the Floquet exponents of Γ) and not by the eigenvalues of R. We therefore analyze the orientability of the bundles depending on the eigenvalues of B.

Remark 2.3 (Orientation of the bundle based on the eigenvalues of B). Let μ an eigenvalue of B together with an associated eigenvector w. We consider three cases.

- ($\mu \in \mathbb{R}$). The associated Floquet multiplier is real and given by $\phi = e^{\mu\tau} > 0$. Therefore the associated eigenvector $w(\theta) = Q(\theta)w$ is not flipped over the interval $[0, \tau]$.
- ($\mu = \nu + \frac{i\pi}{\tau} \in \mathbb{C}$, for a $\nu \in \mathbb{R}$). The associated Floquet multiplier is $\phi = e^{\mu\tau} = e^{\nu\tau}e^{i\pi} = -e^{\nu\tau}$ which is real negative and the orientation of the eigenvector $w(\theta) = Q(\theta)w$ is flipped over $[0, \tau]$. The linear bundle is a Mobius strip. The presence of the twist cannot be inferred from the eigenvalues of R, but rather from the eigenvalues of B. We show in Remark 2.16 how the parameterization handles non-orientability.
- ($\mu = \alpha \pm i\beta \in \mathbb{C}$ not of the form 2.). In this case, the associated Floquet multiplier is complex and the dynamics in the linear bundle is rotational. We will not cover this case, and for more details, we refer to [14].

2.2 Invariance equation

In this section we study an equation which characterizes chart maps for the local invariant stable/unstable manifold, denoted by $W^s_{\text{loc}}(\Gamma)$ and $W^u_{\text{loc}}(\Gamma)$ respectively. The chart maps studied here have the additional property that they conjugate the dynamics on the manifold to a certain linear dynamical system. Throughout this section, we discuss only the stable manifold. The unstable manifold is obtained by reversing time.

Let $f : \mathbb{R}^d \to \mathbb{R}^d$ be a real analytic vector field and suppose γ is a τ-periodic solution of $\dot{x} = f(x)$ and let $\Gamma = \{\gamma(t) : t \in [0, \tau]\}$ the corresponding periodic orbit. Denote by $\mathbb{T}_{2\tau} = [0, 2\tau]_{/\{0,2\tau\}}$ the circle of length 2τ. Let $\varphi\colon \mathbb{R}^d \times \mathbb{R}^+ \to \mathbb{R}^d$ denote the flow generated by f. We assume without loss of generality that φ is globally well-defined. Suppose that Γ is hyperbolic and consider $\Phi(t) = Q(t)e^{Rt}$ the real Floquet normal form of the fundamental matrix solution of the variational system (1). Assume that the matrix R is diagonalizable. Let $\lambda_1, \ldots, \lambda_{d_m} \in \mathbb{C}$ denote the stable eigenvalues of the matrix R, that is $\text{Re}(\lambda_i) < 0$ for all $i = 1, \ldots, d_m$, and let $w_1, \ldots, w_{d_m}$ the associated linearly independent eigenvectors. By invertibility of $Q(\theta)$ for all θ, we have that the associated eigenvectors $w_i(\theta) = Q(\theta)w_i$ are linearly independent for all θ. The stable normal bundle of Γ is then parameterized by

$$\mathbb{P}_1(\theta, \sigma) = \gamma(\theta) + \sum_{i=1}^{d_m} w_i(\theta)\sigma_i, \qquad \theta \in \mathbb{T}_{2\tau} \text{ and } \sigma = (\sigma_1, \ldots, \sigma_{d_m}) \in \mathbb{R}^{d_m},$$

that is $E_s = \text{image}\,(\mathbb{P}_1)$. One goal now is to find a nonlinear correction to $\mathbb{P}_1$ which results in a parameterization of the local stable manifold. In fact we obtain something stronger.

Suppose for the moment that the eigenvalues of R are real and distinct with $\lambda_{d_m} < \ldots < \lambda_1 < 0$. The casesof complex conjugates eigenvalues is similar and discussed in Remark 2.15. The case of repeated eigenvalues is not discussed in the present work, however the reader interested in degeneracies can refer to paper [45]. We consider the vector field

$$\dot{\theta} = 1, \quad \dot{\sigma} = \Lambda \cdot \sigma, \qquad \Lambda \stackrel{\text{def}}{=} \begin{pmatrix} \lambda_1 & & \\ & \ddots & \\ & & \lambda_{d_m} \end{pmatrix}. \tag{5}$$

Let

$$B_\nu \stackrel{\text{def}}{=} \left\{ \sigma \in \mathbb{R}^{d_m} \mid \max_{1 \le i \le d_m} |\sigma_i| \le \nu \right\}.$$

We refer to the cylinder $\mathbb{C}_{2\tau,\nu} \stackrel{\text{def}}{=} \mathbb{T}_{2\tau} \times B_\nu$ as *the parameter space* for the local invariant manifold. Note that the $\sigma = 0$ set is an invariant circle for (5). Also note that the vector field given by (5) is inflowing on the parameter cylinder, that is for any $(\theta, \sigma) \in \partial\,\mathbb{C}_{2\tau,\nu}$ we have that the vector $(1, \Lambda\sigma)$ points inward toward the center of the cylinder. (This is the only place where we exploit that the eigenvalues are real distinct).

We have that the flow on the cylinder is given explicitly by the formula

$$\mathfrak{L}(\theta, \sigma, t) \stackrel{\text{def}}{=} \begin{bmatrix} \theta + t \\ e^{\Lambda t}\sigma \end{bmatrix}, \tag{6}$$

and this flow clearly maps $\mathbb{C}_{2\tau,\nu}$ into its own interior for any $t > 0$, with the circle $\sigma = 0$ a periodic orbit of period 2τ. We take the flow $\mathfrak{L}$ as the "model dynamics" on the stable manifold and look for a chart map which conjugates the nonlinear dynamics on $W^s_{\text{loc}}(\Gamma)$ to the linear dynamics on $\mathbb{C}_{2\tau,\nu}$ given by $\mathfrak{L}$. More precisely we have the following definition.

Definition 2.4 (Conjugating chart map for the local stable manifold). We say that the function $\mathbb{P}\colon \mathbb{T}_{2\tau} \times B_\nu \to \mathbb{R}^d$ is a *conjugating chart map* for a local stable manifold of the periodic orbit Γ if

1. $\mathbb{P}$ is a continuous, surjective mapping of the cylinder $\mathbb{C}_{2\tau,\nu}$ which is real analytic on the interior of the cylinder.
2. $\mathbb{P}(\theta, 0) = \gamma(\theta)$,
3. The conjugacy relation

$$\varphi\left[\mathbb{P}(\theta, \sigma), t\right] = \mathbb{P}\left(\theta + t, e^{\Lambda t}\sigma\right), \tag{7}$$

is satisfied for all $\theta \in \mathbb{T}_{2\tau}$, $\sigma \in B_\nu$, and $t \geq 0$.

Remark 2.5. It might be more correct to call $\mathbb{P}$ a covering map for the manifold rather than a chart map, as the model space is a cylinder rather than a Euclidean space. However in the present work we apply the term "chart" somewhat liberally and trust that no confusion ensues.

The definition asks that $\mathbb{P}$ conjugates the flow generated by the vector field f to the linear flow generated by (6). If $\mathbb{P}$ is a conjugating chart map then for any $(\theta, \sigma) \in \mathbb{C}_{2\tau,\nu}$,

$$\begin{aligned} \lim_{t\to\infty} \|\varphi[\mathbb{P}(\theta,\sigma), t] - \gamma(\theta + t)\| &= \lim_{t\to\infty} \left\|\mathbb{P}\left(\theta + t, e^{\Lambda t}\sigma\right) - \gamma(\theta + t)\right\| \\ &= \lim_{t\to\infty} \|\mathbb{P}\left(\theta + t, 0\right) - \gamma(\theta + t)\| \\ &= 0 \end{aligned} \tag{8}$$

by continuity of $\mathbb{P}$, the conjugacy relation (7) and the contractiveness of $e^{\Lambda t}$. Hence, the orbit of a point in the image of $\mathbb{P}$ accumulates to the periodic orbit Γ with matching asymptotic phase θ. $\mathbb{P}$ is one-to-one and its image is a d_m dimensional manifold (immersed cylinder). Since image($\mathbb{P}$) is an immersed cylinder containing Γ in its interior and having that each of its points accumulates on Γ under the forward flow, image($\mathbb{P}$) is a local stable manifold for Γ.

The following provides sufficient conditions for the existence of a conjugating chart map.

Theorem 2.6 (Invariance equation for a conjugating chart map). *Suppose that $\mathbb{P}\colon \mathbb{T}_{2\tau} \times B_\nu \to \mathbb{R}^d$ is a continuous function such that*

$$\mathbb{P}(\theta, 0) = \gamma(\theta), \qquad \textit{for all } \ \theta \in \mathbb{T}_{2\tau}, \tag{9}$$

$\mathbb{P}$ *is differentiable on the circle* $\sigma = 0$ *with*

$$\frac{\partial}{\partial \sigma_i}\mathbb{P}(\theta, 0) = w_i(\theta), \qquad \text{for each } \; 1 \leq i \leq d_m, \tag{10}$$

and $\mathbb{P}(\theta, \sigma)$ *solves the partial differential equation*

$$\frac{\partial}{\partial \theta}\mathbb{P}(\theta, \sigma) + \sum_{i=1}^{d_m} \lambda_i \sigma_i \frac{\partial}{\partial \sigma_i}\mathbb{P}(\theta, \sigma) = f(\mathbb{P}(\theta, \sigma)), \tag{11}$$

on the interior of $\mathbb{C}_{2\tau,\nu}$. *Then* $\mathbb{P}$ *is a conjugating chart map for* Γ *in the sense of Definition 2.4. It follows from (8) that image*$(\mathbb{P})$ *is a local stable manifold for* Γ.

Proof. To see that $\mathbb{P}$ is a conjugating chart map choose $(\theta_0, \sigma_0) \in \mathbb{C}_{2\tau,\nu}$, recall (6) and define the curve $x\colon [0, \infty) \to \mathbb{R}^d$ by

$$x(t) = \mathbb{P}(\theta_0 + t, e^{\Lambda t}\sigma_0) = \mathbb{P}(\mathfrak{L}(\theta_0, \sigma_0, t)).$$

Denote $\sigma_0 = (\sigma_1^0, \ldots, \sigma_{d_m}^0) \in B_\nu$. Note that $x(t) \in \text{image}(\mathbb{P})$ for all $t \geq 0$, as $\mathfrak{L}$ is contracting on $\mathbb{C}_{2\tau,\nu}$. Next we show that $x(t)$ solves the initial value problem

$$x'(t) = f(x(t)), \qquad x(0) = \mathbb{P}(\theta_0, \sigma_0), \tag{12}$$

in forward time. To see this note that

$$\begin{aligned} x'(t) &= \frac{d}{dt}\mathbb{P}(\theta_0 + t, e^{\Lambda t}\sigma_0) \\ &= D_{\theta,\sigma}\mathbb{P}(\theta_0 + t, e^{\Lambda t}\sigma_0) \begin{bmatrix} 1 \\ e^{\Lambda t}\Lambda\sigma_0 \end{bmatrix} \\ &= \frac{\partial}{\partial \theta}\mathbb{P}(\theta_0 + t, e^{\Lambda t}\sigma_0) + \sum_{i=1}^{d_m} \frac{\partial}{\partial \sigma_i}\mathbb{P}(\theta_0 + t, e^{\Lambda t}\sigma_0)\lambda_i e^{\lambda_i t}\sigma_i^0. \end{aligned}$$

Now define the new variables $\hat{\sigma}_i = e^{\lambda_i t}\sigma_i^0$ for $1 \leq i \leq d_m$ and $\hat{\theta} = (\theta_0 + t)_{\text{mod } 2\tau}$. Then for any $t > 0$ we have that $(\hat{\theta}, \hat{\sigma}) \in \text{interior}\,(\mathbb{C}_{2\tau,\nu})$. Since (11) holds on the interior by hypothesis we now have that

$$\begin{aligned} \frac{\partial}{\partial \theta}\mathbb{P}(\theta_0 + t, e^{\Lambda t}\sigma_0) + \sum_{i=1}^{d_m} \frac{\partial}{\partial \sigma_i}\mathbb{P}(\theta_0 + t, e^{\Lambda t}\sigma_0)\lambda_i e^{\lambda_i t}\sigma_i^0 &= \frac{\partial}{\partial \theta}\mathbb{P}(\hat{\theta}, \hat{\sigma}) + \sum_{i=1}^{d_m} \frac{\partial}{\partial \sigma_i}\mathbb{P}(\hat{\theta}, \hat{\sigma})\lambda_i \hat{\sigma}_i \\ &= f\left(\mathbb{P}(\hat{\theta}, \hat{\sigma})\right). \end{aligned}$$

But $\mathbb{P}(\hat{\theta}, \hat{\sigma}) = x(t)$, so this shows that $x'(t) = f(x(t))$ for all $t > 0$ as desired. Since $x(0) = P(\theta_0, \sigma_0)$ by definition we indeed have that $P(\theta_0 + t, e^{\Lambda t}\sigma_0)$ solves (12). But (θ_0, σ_0) was arbitrary in $\mathbb{C}_{2\tau,\nu}$, so this shows that

$$x(t) = \mathbb{P}(\theta + t, e^{\Lambda t}\sigma) = \varphi\left[\mathbb{P}(\theta, \sigma), t\right],$$

and $\mathbb{P}$ satisfies (7) on $\mathbb{C}_{2\tau,\nu}$. Then $\mathbb{P}$ satisfies condition 3 of Definition 2.4. We now establish parts 1 and 2 of Definition 2.4. Since f is real analytic and $\mathbb{P}$ solves the differential equation (11), we have that $\mathbb{P}$ is real analytic in the interior of $\mathbb{C}_{2\tau,\nu}$. From (10) we have that

$$D_\sigma \mathbb{P}(\theta, 0) = [w_1(\theta)| \ldots |w_{d_m}(\theta)].$$

This matrix has full rank because the eigenvectors are linearly independent over $\mathbb{T}_{2\tau}$. Since $\mathbb{P}$ is real analytic it is certainly continuously differentiable, and the continuity of the derivative implies that the differential is full rank in a neighborhood of γ, that is there is an $r > 0$ so that $\|\sigma\| \leq r$ implies that $D_\sigma \mathbb{P}(\theta, \sigma)$ is full rank. If follows from the implicit function theorem that $\mathbb{P}$ is injective for $\|\sigma\| < r$.

Now consider $(\theta_1, \sigma_1), (\theta_2, \sigma_2) \in \mathbb{C}_{2\tau,\nu}$ and suppose that

$$\mathbb{P}(\theta_1, \sigma_1) = \mathbb{P}(\theta_2, \sigma_2). \tag{13}$$

Since $e^{\Lambda t} \to 0$ as $t \to \infty$ there exists $\hat{t} > 0$ such that

$$\left\| e^{\Lambda \hat{t}} \sigma_1 \right\|, \left\| e^{\Lambda \hat{t}} \sigma_2 \right\| < r. \tag{14}$$

Since $\mathbb{P}$ satisfies the conjugacy equation (7) we have that

$$\mathbb{P}\left(\theta_1 + \hat{t}, e^{\Lambda \hat{t}} \sigma_1\right) = \varphi\left(\mathbb{P}(\theta_1, \sigma_1), \hat{t}\right), \quad \text{and} \quad \mathbb{P}\left(\theta_2 + \hat{t}, e^{\Lambda \hat{t}} \sigma_2\right) = \varphi\left(\mathbb{P}(\theta_2, \sigma_2), \hat{t}\right).$$

From (13) (as well as the uniqueness of trajectories under φ) it follows that

$$\mathbb{P}\left(\theta_1 + \hat{t}, e^{\Lambda \hat{t}} \sigma_1\right) = \mathbb{P}\left(\theta_2 + \hat{t}, e^{\Lambda \hat{t}} \sigma_2\right).$$

It follows from the conditions of (14) and the fact that $\mathbb{P}$ is injective on $\mathbb{T}_{2\tau} \times B_r$ that

$$\left(\theta_1 + \hat{t}, e^{\Lambda \hat{t}} \sigma_1\right) = \left(\theta_2 + \hat{t}, e^{\Lambda \hat{t}} \sigma_2\right).$$

Since the linear flow map is invertible at $\hat{t}$ we have that $(\theta_1, \sigma_1) = (\theta_2, \sigma_2)$ and $\mathbb{P}$ is an injection of $\mathbb{C}_{2\tau,\nu}$ into $\mathbb{R}^d$. Then $\mathbb{P}$ is a conjugating chart map for the stable manifold of γ as desired. □

Definition 2.7. We call equation (11) from Theorem 2.6 the *invariance equation*.

Remark 2.8. The converse of Theorem 2.6 holds. Indeed if $\mathbb{P}$ satisfies (9), (10), and in addition is a differentiable conjugating chart map in the sense of Definition 2.4, then $\mathbb{P}$ is a solution of the partial differential equation (11). To see this one differentiates the conjugacy equation (7) with respect to time, and takes the limit as $t \to 0$ in the resulting expression to recover (11). Then (11) subject to the first order constraints (9) and (10) constitute necessary and sufficient conditions for the existence of a conjugating chart map parameterizing a local stable manifold for Γ. The length of the eigenvectors is unspecified throughout this discussion, and it follows that the conjugating chart map $\mathbb{P}$ is unique up to the choice of this scaling.

The preceding discussion shows that in order to study the local invariant manifolds of Γ it is enough to study (11), appropriately constrained. The following provides a necessary condition for the existence of solutions of equation (11), in terms of certain algebraic constraints between the stable eigenvalues.

Definition 2.9 (Resonant eigenvalues). We say that the stable eigenvalues $\lambda_1, \ldots, \lambda_{d_m}$ of R are *resonant* at order $\alpha \in \mathbb{N}^{d_m}$ if there is a $1 \leq i \leq d_m$ so that

$$\alpha_1 \lambda_1 + \ldots + \alpha_{d_m} \lambda_{d_m} - \lambda_i = 0. \tag{15}$$

Lemma 2.10 (Divergence Theorem). If there is a resonance in the sense of Definition 2.9 at some order $|\alpha| = \alpha_1 + \cdots + \alpha_{d_m} \geq 2$ then the invariance equation (11) has no solution.

The proof follows from the computations in Section 2.4. In particular see Remark 2.13 and also [47].

So, Lemma 2.10 provides conditions under which we fail to have solutions of the invariance equation (11). Also observe that there can be no resonances of order $\alpha \in \mathbb{N}^{d_m}$ when

$$2 \leq |\alpha| \leq \left\lceil \frac{\mathrm{Re}(\lambda_{d_m})}{\mathrm{Re}(\lambda_1)} \right\rceil,$$

that is α is eventually large enough that (15) cannot hold as $\mathrm{Re}(\lambda_1), \ldots, \mathrm{Re}(\lambda_{d_m})$ have the same sign. Then in fact there are only a finite number of possible resonances, and this finite number is determined by the "spectral gap" (ratio of the largest and smallest real part taken over the set of stable eigenvalues). For a more thorough discussion of resonances see [45, 46, 47, 59, 62].

2.3 Homological equations

In this section we develop a formal series solution for equation (11). Explicitly we assume a series solution of the form

$$\mathbb{P}(\theta, \sigma) = \sum_{|\alpha|=0}^{\infty} a_\alpha(\theta)\sigma^\alpha = \sum_{|\alpha|=0}^{\infty} \sum_{k \in \mathbb{Z}} a_{\alpha,k} e^{\frac{2\pi i}{2\tau} k\theta} \sigma^\alpha. \tag{16}$$

Here $\alpha \in \mathbb{N}^{d_m}$ is a d_m-dimensional multi-index, $a_{\alpha,k} \in \mathbb{R}^d$ for all α, k, $|\alpha| = \alpha_1 + \cdots + \alpha_{d_m}$ and $\sigma^\alpha = \sigma_1^{\alpha_1} \cdots \sigma_{d_m}^{\alpha_{d_m}}$. We refer to expansion (16) as a *Fourier-Taylor series*. We substitute (16) into the invariance equation (11) and expand the vector field $f(\mathbb{P}(\theta, \sigma))$ as its Taylor series with respect to the variable σ evaluated at $\sigma = 0$, that is

$$f(\mathbb{P}(\theta, \sigma)) = f(\mathbb{P}(\theta, 0)) + \sum_{i=1}^{d_m} \frac{\partial}{\partial \sigma_i} f(\mathbb{P}(\theta, 0))\sigma_i + \sum_{|\alpha| \geq 2} \frac{1}{\alpha!} f^{(\alpha)}(\mathbb{P}(\theta, 0))\sigma^\alpha,$$

where $f^{(\alpha)}(\mathbb{P}(\theta, 0))$ is the derivative $\frac{\partial^{|\alpha|}}{\partial \sigma^\alpha} f(\mathbb{P}(\theta, \sigma))$ evaluated at $\sigma = 0$. Then we collect the terms with the same power of σ and we solve the resulting equations. Since

$$\frac{\partial}{\partial \theta}\mathbb{P}(\theta, \sigma) = \sum_{|\alpha| \geq 0} \Big(\frac{d}{d\theta} a_\alpha(\theta)\Big)\sigma^\alpha, \qquad \frac{\partial}{\partial \sigma_i}\mathbb{P}(\theta, \sigma) = \sum_{|\alpha| > 0} a_\alpha \alpha_i \sigma^\alpha \sigma_i^{-1},$$

we end up with the following sequence of differential equations.

$|\alpha| = 0$: The only multi-index with zero length is $\mathbf{0} = (0, \ldots, 0)$. The term in $\sigma^{\mathbf{0}}$ gives

$$\frac{d}{d\theta} a_{\mathbf{0}}(\theta) = f(a_{\mathbf{0}}(\theta))$$

whose solution is given by the periodic orbits itself, hence $a_{\mathbf{0}}(\theta) = \gamma(\theta)$.

$|\alpha| = 1$: The multi-indices of length 1 are $e_i = (0, \ldots, 1, \ldots, 0)$ with 1 in the i-th position. Since $\frac{\partial}{\partial \sigma_i} f(\mathbb{P}(\theta, 0))\sigma_i = Df(a_{\mathbf{0}}(\theta))a_{e_i}(\theta)$, equating the terms in σ^{e_i} for each $i = 1, \ldots, d_m$ yields

$$\begin{cases} \dfrac{d}{d\theta} a_{e_i}(\theta) + \lambda_i a_{e_i}(\theta) = Df(a_{\mathbf{0}}(\theta))a_{e_i}(\theta) \\ \\ \lambda_i \in \mathbb{R},\ a_{e_i}(\theta)\ 2\tau-\text{periodic}. \end{cases} \tag{17}$$

$|\alpha| \geq 2$: Once $a_{\mathbf{0}}(\theta)$ and $a_{e_i}(\theta)$ are given, we obtain equations of the form

$$\frac{da_\alpha(\theta)}{d\theta} + (\alpha_1\lambda_1 + \ldots + \alpha_{d_m}\lambda_{d_m})a_\alpha(\theta) = Df(a_{\mathbf{0}}(\theta))a_\alpha(\theta) + \boldsymbol{R}_\alpha(\theta), \tag{18}$$

where $\boldsymbol{R}_\alpha$ involves only lower order terms. Equation (18) is referred to as the *homological equation* for the coefficient $a_\alpha(\theta)$ with $|\alpha| \geq 2$. In case the nonlinearities in $f(x)$ are polynomials, the computation of the remaining terms $\boldsymbol{R}_\alpha$ can be done easily by means of the Cauchy products. Indeed the polynomials coincide with the Taylor polynomials.

We now show that all solutions to (17) are given by $(\lambda_i, a_{e_i}(\theta)) = (\lambda_i, Q(\theta)w_i)$ where (λ_i, w_i) is any eigenpair of R appearing in (2). Given a matrix A, denote by $\Sigma(A)$ the set of all (λ, v) such that $Av = \lambda v$.

Proposition 2.11. *Let $\Phi(t) = Q(t)e^{Rt}$ be the real Floquet normal form decomposition of the fundamental matrix solution of system (1). Then all the solutions $(\lambda_i, a_{e_i}(\theta))$ of (17) are given by $(\lambda_i, Q(\theta)w_i)$ with $(\lambda_i, w_i) \in \Sigma(R)$.*

Proof. For any λ, the function $\Phi_\lambda(\theta) = \Phi(\theta)e^{-\lambda\theta}$ is the fundamental matrix solution of $\dot{x} = Df(\gamma(t))x - \lambda x$. Indeed

$$\dot{\Phi}_\lambda(\theta) = \dot{\Phi}e^{-\lambda\theta} - \lambda\Phi(\theta)e^{-\lambda\theta} = Df(\gamma(\theta))\Phi(\theta)e^{-\lambda\theta} - \lambda\Phi(\theta)e^{-\lambda\theta} = Df(\gamma(\theta))\Phi_\lambda(\theta) - \lambda\Phi_\lambda(\theta)$$

and $\Phi_\lambda(0) = I$. Let $(\lambda_i, w_i) \in \Sigma(R)$ and let $a_{e_i}(\theta) \stackrel{\text{def}}{=} \Phi_{\lambda_i}(\theta)w_i$. Thus $(\lambda_i, a_{e_i}(\theta))$ is a solution of (17). Moreover, since (λ_i, w_i) is an eigenpair of R, it follows that

$$a_{e_i}(\theta) = \Phi(\theta)e^{-\lambda_i\theta}w_i = e^{-\lambda_i\theta}Q(\theta)e^{R\theta}w_i = e^{-\lambda_i\theta}Q(\theta)e^{\lambda_i\theta}w_i = Q(\theta)w_i$$

proving that $a_{e_i}(\theta)$ is 2τ-periodic. We conclude that $(\lambda_i, Q(\theta)w_i)$ is a solution of (17).

On the contrary, suppose $(\lambda_i, a_{e_i}(\theta))$ is a solution of problem (17). Thus

$$a_{e_i}(\theta) = \Phi_{\lambda_i}(\theta)a_{e_i}(0) = \Phi(\theta)e^{-\lambda_i\theta}a_{e_i}(0).$$

Since $a_{e_i}(\theta)$ is 2τ-periodic, $a_{e_i}(0) = a_{e_i}(2\tau) = \Phi(2\tau)e^{-\lambda_i 2\tau}a_{e_i}(0)$, that is $(e^{2\lambda_i\tau}, a_{e_i}(0)) \in \Sigma(\Phi(2\tau))$. From the real Floquet normal form decomposition (2), we have that $\Phi(2\tau) = Q(2\tau)e^{2\tau R} = e^{2\tau R}$. Moreover, the spectrum of R is in one-to-one correspondence with the spectrum of $\Phi(2\tau)$ since $(\lambda, w) \in \Sigma(R)$ if and only if $(e^{2\tau\lambda}, w) \in \Sigma(\Phi(2\tau))$. We conclude that $a_{e_i}(0) = w_i$ and $(\lambda_i, w_i) \in \Sigma(R)$. From this it follows that $a_{e_i}(\theta) = Q(\theta)w_i$. □

The existence of 2τ-periodic solutions of (18) is discussed in the following result whose proof can be found in [47].

Theorem 2.12. *If $e^{2\nu\tau}$ is not an eigenvalue of $\Phi(2\tau)$ then, for any 2τ-periodic function $\boldsymbol{R}_\alpha$, there exists a 2τ-periodic solution a_α of $(\frac{d}{d\theta} - Df(a_{\mathbf{0}}) + \nu)a_\alpha = \boldsymbol{R}_\alpha$.*

Taking $\nu = \alpha_1\lambda_1 + \ldots + \alpha_{d_m}\lambda_{d_m}$, if $e^{2(\alpha_1\lambda_1+\ldots+\alpha_{d_m}\lambda_{d_m})\tau}$ is not an eigenvalue of $\Phi(2\tau)$, there exist 2τ-periodic functions $a_\alpha(\theta)$ solutions of (18). That comes from the previous theorem and from the fact that the remaining term $\boldsymbol{R}_\alpha$ is 2τ-periodic.

2.4 Efficient solution of the homological equations: reducibility via the Floquet normal form

The situation encountered in Section 2.3, namely where one is trying to solve an invariance equation for a conjugating map and finds that the problem reduces to solving infinitely many

linear equations, is not uncommon. It arises frequently in the study of normal forms (e.g. see [37, 77]). As often happens in normal form theory we find that solving the resulting system of infinitely many linear differential equations is nontrivial, and seek further reduction.

For example when studying conjugating maps and normal forms for invariant objects in Hamiltonian dynamical systems it is sometimes possible to exploit the preservation of geometric structure in order to obtain a change of coordinates which reduces the homological equations to constant coefficient (or perhaps to constant coefficient plus a quadratically small error). We refer to [64] for a more complete elaboration on this theme. The interested reader can also refer to [65] for a discussion of computing invariant tori in Hamiltonian systems without the use of action angle variables. [82, 83] use these ideas to compute invariant tori in volume preserving systems. See [57] for an example involving invariant manifolds for fixed points having some stable and some unstable directions in both symplectic and volume preserving systems. Another recent advance in this direction has been the extension of KAM theory to certain dissipative systems which preserve a conformally symplectic structure [76].

The point of these examples is that the choice of an appropriate coordinate system greatly simplifies the study and computation of invariant objects in dynamical systems theory. In this section we observe that reducibility for the problem of parameterizing the stable/unstable manifold of a non-resonant hyperbolic periodic orbit is achieved using a coordinate change given by the Floquet normal form (2). We will see that the homological equations (18) are reduced to *diagonal constant coefficient in Fourier space*, and this leads to particularly simple equations for the Fourier-Taylor coefficients for the desired conjugating chart map. One may contrast this to the approach of [71, 72] where the homological equations (18) are solved for planar systems without using the Floquet normal form.

In order to formalize this, recall that Q from (2) is a solution of the differential equation

$$Q'(\theta) + Q(\theta)R = Df(\gamma(\theta))Q(\theta) \tag{19}$$

with R a real-valued matrix. We assume that R is diagonalizable, that is that there exists M such that

$$R = M\Sigma M^{-1},$$

with

$$\Sigma = \begin{pmatrix} \Lambda_s & 0 & 0 \\ 0 & \Lambda_u & 0 \\ 0 & 0 & 0 \end{pmatrix}.$$

Here Λ_s is the $d_m \times d_m$ diagonal matrix of eigenvalues with negative real parts and Λ_u is the diagonal matrix of eigenvalues with positive real parts. As before $w_1, \ldots, w_{d_m}$ are the linearly independent eigenvectors associated with the stable eigenvalues. Again the functions $w_j(\theta) = Q(\theta)w_j$ parameterize the stable invariant normal bundle.

We will now see that the homological equation (18) is reduced to constant coefficient by the Floquet normal form. For $|\alpha| \geq 2$ define the functions $w_\alpha(\theta) : \mathbb{T}_{2\tau} \to \mathbb{R}^d$ by the coordinate transformation

$$a_\alpha(\theta) = Q(\theta)w_\alpha(\theta).$$

Taking into account (19), the homological equation (18) is transformed into the constant coefficient ordinary differential equation

$$\frac{d}{d\theta}w_\alpha(\theta) + ((\alpha_1\lambda_1 + \ldots + \alpha_{d_m}\lambda_{d_m})I - R)\, w_\alpha(\theta) = Q^{-1}(\theta)\boldsymbol{R}_\alpha(\theta). \tag{20}$$

We now expand w_α as

$$w_\alpha(\theta) = \sum_{k\in\mathbb{Z}} w_{\alpha,k} e^{\frac{2\pi i k}{2\tau}\theta}, \qquad (w_{\alpha,k} \in \mathbb{C}^d)$$

and

$$Q^{-1}(\theta)\boldsymbol{R}_\alpha(\theta) = \sum_{k\in\mathbb{Z}} A_{\alpha,k} e^{\frac{2\pi i k}{2\tau}\theta}, \qquad (A_{\alpha,k} \in \mathbb{C}^d).$$

We make a final coordinate transformation and define $v_{\alpha,k}$ by

$$w_{\alpha,k} = M v_{\alpha,k}.$$

Then equation (20) gives

$$v_{\alpha,k} = \left[\left(\frac{2\pi i k}{2\tau} + \alpha_1\lambda_1 + \ \ldots + \alpha_{d_m}\lambda_{d_m} \right) I - \Sigma \right]^{-1} M^{-1} A_{\alpha,k}.$$

But this is diagonalized and solving component-wise we obtain

$$v^{(j)}_{\alpha,k} = \frac{1}{\frac{2\pi i k}{2\tau} + \alpha_1\lambda_1 + \ldots + \alpha_{d_m}\lambda_{d_m} - \lambda_j} (M^{-1}A_{\alpha,k})^{(j)}, \tag{21}$$

for $1 \le j \le d_m$. Working backward from $v_\alpha(\theta)$ we obtain the desired solution $a_\alpha(\theta)$ by

$$a_\alpha(\theta) = Q(\theta) M v_\alpha(\theta). \tag{22}$$

Remark 2.13 (**Resonances revisited).** The Fourier-Taylor coefficients $v^{(j)}_{\alpha,k}$ defined by (21) are formally well defined to all orders precisely when there are no resonances in the sense of Definition 2.9. This fact establishes Lemma 2.10.

Remark 2.14 (**Efficient numerical computations).** If the Fourier coefficients for both the periodic solution $\gamma(\theta)$ and $Q(\theta)$ are known, then the recurrence equations given in (21) combined with the coordinate transformation given by (22) provide a recipe for computing the conjugating chart map $\mathbb{P}(\theta, \sigma)$ to any desired finite order. This is how we obtain the numerical approximations used in Sections 3 and 4. To compute the Floquet normal form, we can use the theory developed in [80]. This assumes that the form of the functions $\boldsymbol{R}_\alpha(\theta)$ are known explicitly. In Section 2.5 we illustrate this computation for the Lorenz system.

Remark 2.15 (**The case of complex conjugates eigenvalues of $\boldsymbol{R}$).** Assume that $\lambda_{1,2} = a \pm ib$ are eigenvalues of the matrix R coming from the Floquet normal form (2). For sake of simplicity of the presentation, assume that $d_m = 2$. In this case we still conjugate to the flow given by (7), however we do not obtain real results when we flow by

$$e^{\Lambda t}\sigma = \exp\left(\begin{bmatrix} a+ib & 0 \\ 0 & a-ib \end{bmatrix} t \right) \begin{bmatrix} \sigma_1 \\ \sigma_2 \end{bmatrix}.$$

Because of this the coefficients of the parameterization $\mathbb{P}$ will not be real either. Note however that the linear flow still takes complex conjugate arguments to complex conjugate results. This property is then inherited by the parameterization coefficients and is then exploited to obtain a real result. Making the usual complex conjugate variables $\sigma_1 = t + is$ and $\sigma_2 = t - is$ we observe, by considering the recurrence equations (21), that the coefficients a_{α_1,α_2} for the parameterization have that property that $a_{\alpha_1,\alpha_2}(\theta) = \overline{a_{\alpha_2,\alpha_1}(\theta)}$. Then, as long as we have chosen complex conjugate eigenvectors, the complex conjugate change of variables are precisely what is needed in order to obtain a real valued function, that is

$$\mathbb{P}(\theta, s+it, s-it) \in \mathbb{R}^d$$

for all θ, s, t. This is the same idea used in [55, 56, 60] in order to parameterize real invariant manifolds associated with fixed points when there are complex conjugate eigenvalues. See the works just cited for more thorough discussion. The case $d_m > 2$ is similar.

Remark 2.16 (The parameterization and non-orientability of the manifold). Note that even if the stable/unstable manifold is non-orientable, the τ-periodic orbit Γ is a τ-periodic geometrical object. Then the 2τ-periodic parametrization $\mathbb{P}(\theta,\sigma)$ should cover twice the same manifold. In general, we then have two possibilities:

$$\mathbb{P}(\theta+\tau,\sigma)=\mathbb{P}(\theta,\sigma) \qquad \text{or} \qquad \mathbb{P}(\theta+\tau,\sigma)=\mathbb{P}(\theta,-\sigma).$$

The first possibility is when $Q(t)$ is τ-periodic in which case the normal bundle is orientable. If the normal bundle is non-orientable, then we are in the second case. More precisely, the relation $\mathbb{P}(\theta+\tau,\sigma)=\mathbb{P}(\theta,-\sigma)$ implies that

$$\sum_{n\geq 0} a_n(\theta+\tau)\sigma^n=\sum_{n\geq 0} a_n(\theta)(-\sigma)^n.$$

Therefore, $a_n(\theta+\tau)=a_n(\theta)$ for n even and $a_n(\theta+\tau)=-a_n(\theta)$ for n odd, that is a_n is τ-periodic for n even and a_n is 2τ-periodic but odd in $\theta=\tau$ for odd n, a relation that $a^0=\gamma$ and a^1 satisfy. In practice our computations result in a sequence of a_n with exactly the above properties. Thus we can restrict to positive σ and $\theta\in[0,2\tau]$ or $\sigma\in[-\delta,\delta]$ and $\theta\in[0,\tau]$ in order to parameterize the complete manifold.

2.5 Explicit solution of the homological equations in Lorenz

The full computation of the homological equations, including the derivation of the precise form of the right-hand-sides $\boldsymbol{R}_\alpha(\theta)$ is best illustrated in the context of specific examples. To this end, recall that the Lorenz equations are given by the quadratic vector field

$$f(x,y,z)=\begin{pmatrix} -sx+sy \\ \rho x-y-xz \\ -\beta z+xy \end{pmatrix}, \qquad (s,\beta,\rho\in\mathbb{R}). \tag{23}$$

We expand the τ-periodic solution γ by considering it as a 2τ-periodic function, and consider the Fourier expansion of the 2τ-periodic matrix Q from (2), that is

$$\gamma(\theta)=\sum_{k\in\mathbb{Z}}\gamma_k e^{\frac{2\pi i k}{2\tau}\theta} \qquad \text{and} \qquad Q(\theta)=\sum_{k\in\mathbb{Z}} Q_k e^{\frac{2\pi i k}{2\tau}\theta}.$$

Choose $(\lambda,w)\in\Sigma(R)$, $\lambda\neq 0$. In this section, we only consider orbits with one dimensional stable and unstable manifolds. Hence, for each manifold, we seek a function of the form

$$\mathbb{P}(\theta,\sigma)=\sum_{\alpha=0}^{\infty} a_\alpha(\theta)\sigma^\alpha=\sum_{\alpha=0}^{\infty}\sum_{k\in\mathbb{Z}} a_{\alpha,k}e^{\frac{2\pi i k}{2\tau}\theta}\sigma^n. \tag{24}$$

Denote $a_\alpha=(a_\alpha^{(1)},a_\alpha^{(2)},a_\alpha^{(3)})^T\in\mathbb{R}^3$ and $\mathbb{P}=(\mathbb{P}_1,\mathbb{P}_2,\mathbb{P}_3)^T$. Then we require that $\mathbb{P}(\theta,0)=\gamma(\theta)$ and $\frac{\partial}{\partial\theta}\mathbb{P}(\theta,0)=w(\theta)$ and take the Fourier-Taylor coefficients (of Taylor order 0 and 1) to be

$$a_{0,k}=\gamma_k \qquad \text{and} \qquad a_{1,k}=Q_k w,$$

for all $k\in\mathbb{Z}$. This determines the parameterization to first order. In order to determine the higher order coefficients we plug the unknown expansion given by (24) into the invariance equation (11) and obtain

$$\frac{\partial}{\partial\theta}\mathbb{P}(\theta,\sigma)+\lambda\sigma\frac{\partial}{\partial\sigma}\mathbb{P}(\theta,\sigma)=\begin{pmatrix} -s\mathbb{P}_1(\theta,\sigma)+s\mathbb{P}_2(\theta,\sigma) \\ \rho\mathbb{P}_1(\theta,\sigma)-\mathbb{P}_2(\theta,\sigma)-(\mathbb{P}_1\cdot\mathbb{P}_3)(\theta,\sigma) \\ -\beta\mathbb{P}_3(\theta,\sigma)+(\mathbb{P}_1\cdot\mathbb{P}_2)(\theta,\sigma) \end{pmatrix}, \tag{25}$$

where

$$(\mathbb{P}_1 \cdot \mathbb{P}_2)(\theta,\sigma) = \sum_{\alpha=0}^{\infty} p_\alpha^{(1,2)}(\theta)\sigma^\alpha \quad \text{and} \quad (\mathbb{P}_1 \cdot \mathbb{P}_3)(\theta,\sigma) = \sum_{\alpha=0}^{\infty} p_\alpha^{(1,3)}(\theta)\sigma^\alpha,$$

with

$$p_\alpha^{(1,2)}(\theta) \stackrel{\text{def}}{=} \sum_{\substack{\alpha_1+\alpha_2=\alpha \\ \alpha_i \geq 0}}^{\infty} a_{\alpha_1}^{(1)}(\theta) a_{\alpha_2}^{(2)}(\theta) \quad \text{and} \quad p_\alpha^{(1,3)}(\theta) \stackrel{\text{def}}{=} \sum_{\substack{\alpha_1+\alpha_2=\alpha \\ \alpha_i \geq 0}}^{\infty} a_{\alpha_1}^{(1)}(\theta) a_{\alpha_2}^{(3)}(\theta).$$

It is convenient to separate in $p_\alpha^{(i,j)}$ the highest order terms in α, that is

$$\begin{aligned} p_\alpha^{(1,2)}(\theta) &= a_\alpha^{(1)}(\theta) a_0^{(2)}(\theta) + a_0^{(1)}(\theta) a_\alpha^{(2)}(\theta) + \tilde{p}_\alpha^{(1,2)}(\theta) \\ p_\alpha^{(1,3)}(\theta) &= a_\alpha^{(1)}(\theta) a_0^{(3)}(\theta) + a_0^{(1)}(\theta) a_\alpha^{(3)}(\theta) + \tilde{p}_\alpha^{(1,3)}(\theta), \end{aligned}$$

with

$$\tilde{p}_\alpha^{(1,2)}(\theta) \stackrel{\text{def}}{=} \sum_{\substack{\alpha_1+\alpha_2=\alpha \\ \alpha_i > 0}}^{\infty} a_{\alpha_1}^{(1)}(\theta) a_{\alpha_2}^{(2)}(\theta) \quad \text{and} \quad \tilde{p}_\alpha^{(1,3)}(\theta) \stackrel{\text{def}}{=} \sum_{\substack{\alpha_1+\alpha_2=\alpha \\ \alpha_i > 0}}^{\infty} a_{\alpha_1}^{(1)}(\theta) a_{\alpha_2}^{(3)}(\theta).$$

The reason of the last definition stands on the fact that, when matching like powers of σ in the right term of (25), the coefficient of σ^α is given by

$$\begin{pmatrix} -s a_\alpha^{(1)} + s a_\alpha^{(2)} \\ \rho a_\alpha^{(1)} - a_\alpha^{(2)} - p_\alpha^{(1,3)} \\ -\beta a_\alpha^{(3)} + p_\alpha^{(1,2)} \end{pmatrix} = Df(a_0)a_\alpha + \boldsymbol{R}_\alpha(\theta) \stackrel{\text{def}}{=} Df(a_0)a_\alpha + \begin{pmatrix} 0 \\ -\tilde{p}_\alpha^{(1,3)}(\theta) \\ \tilde{p}_\alpha^{(1,2)}(\theta) \end{pmatrix},$$

where the function $\boldsymbol{R}_\alpha(\theta)$ involves only lower order terms. Therefore, matching the coefficients of σ^α in (25), it follows that the functions $a_\alpha(\theta)$ satisfy the differential equations

$$\frac{d}{d\theta} a_\alpha(\theta) + \lambda\alpha a_\alpha(\theta) - Df(\gamma(\theta))a_\alpha(\theta) = \boldsymbol{R}_\alpha(\theta). \tag{26}$$

Here we have used the fact that $a_0(\theta) = \gamma(\theta)$ as well as the analytic expression for $Df(x,y,z)$. Equation (26) is referred to as the *homological equation* for the coefficients of $\mathbb{P}$. Now that $\boldsymbol{R}_\alpha(\theta)$ is known, the parameterization coefficients are computed directly using (21).

Remark 2.17 (**Non-resonance and numerics for Lorenz).**
• In the present situation the denominator in (21) is one of the following

$$\frac{2\pi i k}{2\tau} + \alpha\lambda - \lambda_s, \qquad \frac{2\pi i k}{2\tau} + \alpha\lambda - \lambda_u, \qquad \text{or} \qquad \frac{2\pi i k}{2\tau} + \alpha\lambda,$$

and none of these are ever zero, due to the assumption that Γ is hyperbolic (one stable and one unstable eigenvalue) as well as the condition that $\alpha \geq 2$. Then the solution given by (21) is formally well-defined to all orders. In fact this is always true of a two dimensional stable/unstable manifold of a periodic orbit associated with a single eigendirection: there can be no resonances in this case. This was already shown in [47] without the use of the Floquet theory and exploited for numerical purposes in [71, 72].

• While (21) gives an explicit representation of the components of the k-th Fourier coefficient of the α-th solution function $v_\alpha(\theta)$ for all k and α, the coefficients $A_{\alpha,k}$ are convolution coefficients depending on the coefficients of $\boldsymbol{R}_\alpha$ and Q^{-1}. Then in fact

$$A_{\alpha,k} = \sum_{\ell\in\mathbb{Z}} (\boldsymbol{R}_\alpha)_{k-\ell}(Q^{-1})_\ell,$$

and the coefficients of $\boldsymbol{R}_\alpha$ are themselves convolutions involving lower order terms of $\mathbb{P}$. Since we are dealing with Fourier series all of the convolution sums are infinite series. However in practice we only compute finitely many Fourier coefficients for γ, Q and hence for $\boldsymbol{R}_\alpha$. For example in the Lorenz computations discussed above we have for $\alpha = 2$

$$\boldsymbol{R}_2(\theta) = \begin{pmatrix} 0 \\ -a_1^{(1)}(\theta)a_1^{(3)}(\theta) \\ a_1^{(1)}(\theta)a_1^{(2)}(\theta) \end{pmatrix} = \begin{pmatrix} 0 \\ -w^{(1)}(\theta)w^{(3)}(\theta) \\ w^{(1)}(\theta)w^{(2)}(\theta) \end{pmatrix}.$$

But $w(\theta) = Q(\theta)w = \left(w^{(1)}(\theta), w^{(2)}(\theta), w^{(3)}(\theta)\right)$ is only known numerically up to K modes, hence $\boldsymbol{R}_2(\theta)$ is only computed approximately. Similar comments apply for all $\alpha \geq 2$, so that all $A_{\alpha,k}$ are only known up to a finite number of terms and we only know the functions $v_\alpha(\theta)$ approximately. This makes the a-posteriori analysis discussed in Section 2.6 especially valuable when assessing the quality of the resulting approximation.
• In light of the previous remark we must ask: is the scheme described here at all reasonable? The answer will depend ultimately on the regularity of the vector field f. If f is analytic then γ, Q, and ultimately $\mathbb{P}$ are analytic functions and hence have Fourier-Taylor coefficients which decay exponentially. In this case it is reasonable to expect that some finite number of modes represent the function very well, and that in each convolution term the contributions of higher order modes is not very important. On the other hand if f is less regular then this may not be the case and the procedure may fail. These issues are the subject of paper II. In the present work we focus on analytic vector fields.

2.6 A-posteriori error evaluation

Given a Taylor truncation order $N \in \mathbb{N}$ and a Fourier truncation order $K \in \mathbb{N}$, suppose that

$$\mathbb{P}_{N,K}(\theta,\sigma) \stackrel{\text{def}}{=} \sum_{|\alpha|=0}^{N} \sum_{k=-K}^{K} a_{\alpha,k} e^{\frac{2\pi i}{2\tau}k\theta}\sigma^\alpha,$$

is a candidate solution of equation (1). Here the coefficients $a_{\alpha,k}$ may be computed via the techniques of Section 2.4, or by some other method all together (such as in [71, 72]). The natural question is now "how good is the approximate solution $\mathbb{P}_{N,K}$?" In order to formalize this question we have to decide on the domain of $\mathbb{P}_{N,K}$.
The Question of Domain: *While the global stable/unstable manifold of the periodic orbit Γ is a uniquely defined invariant object, there are many local invariant manifolds. In fact if $\mathbb{P}$ is a chart map for $W^{s,u}_{\text{loc}}(\Gamma)$ and $[0,2\tau]\times U$ is the domain of $\mathbb{P}$, then $\mathbb{P}'$ defined on $[0,2\tau]\times U'$ is a chart map (for a smaller local stable/unstable manifolds) for any $U' \subset U$ containing the origin. Then when we say that $\mathbb{P}_{N,K}$ approximates the parameterization map $\mathbb{P}$ it is essential that we specify the domain on which the comparison is being made.*
The issue is complicated by the fact that $\mathbb{P}_{N,K}$ is a trigonometric polynomial, hence the candidate solution is entire. Yet we do not expect that $\mathbb{P}_{N,K}(\theta,\sigma)$ is a good approximate

solution for all $\|\sigma\| > 0$. Rather we expect that there is a $\nu > 0$ so that the approximation is good in the range $0 < \|\sigma\| \leq \nu$.

We employ the following norm when discussing the Fourier-Taylor series. It is essentially a weighted "little ell one" norm for the space of all sequences of Fourier-Taylor coefficients. Let

$$\|\mathbb{P}\|_{r,\nu}^{W} = \sum_{|\alpha|\geq 0} \sum_{k\in\mathbb{Z}} \|a_{\alpha,k}\| e^{\frac{2\pi|k|}{2\tau}r} \nu^{|\alpha|} \qquad \text{(weighted Wiener-norm)}. \tag{27}$$

If this norm is bounded then $\mathbb{P}$ has a C^0 norm less than $\|\mathbb{P}\|_{r,\nu}^{W}$.

Definition 2.18 (A-posteriori error for equation (11)). Let $\mathbb{P}_{N,K}$ be an approximate solution of the invariance equation (11). Define the *error function* or *defect* associated with $\mathbb{P}_{N,K}$ to be

$$E(\theta,\sigma) \stackrel{\text{def}}{=} \frac{\partial}{\partial\theta}\mathbb{P}_{N,K}(\theta,\sigma) + D_\sigma \mathbb{P}_{N,K}(\theta,\sigma)\Lambda\sigma - f\left(\mathbb{P}_{N,K}(\theta,\sigma)\right),$$

and the a-posteriori error associated with $\mathbb{P}_{N,K}$ on $\mathbb{C}_{2\tau,\nu} = \mathbb{T}_{2\tau} \times B_\nu$ to be

$$\epsilon(r,\nu) \stackrel{\text{def}}{=} \|E\|_{r,\nu}^{W}.$$

Supposing that $f \circ \mathbb{P}_{N,K}$ has Fourier-Taylor expansion

$$f(\mathbb{P}_{N,K})(\theta,\sigma) = \sum_{|\alpha|\geq 0} \sum_{k\in\mathbb{Z}} b_{\alpha,k} e^{\frac{2\pi ik}{2\tau}\theta} \sigma^\alpha,$$

we obtain the explicit formula for the a-posteriori error indicator $\epsilon(r,\nu)$ in Fourier-Taylor space given by

$$\epsilon(r,\nu) = \sum_{|\alpha|\geq 0} \sum_{k\in\mathbb{Z}} \left\| \frac{2\pi ik}{2\tau} a_{\alpha,k} + (\lambda_1\alpha_1 + \ldots + \lambda_k\alpha_k)a_{\alpha,k} - b_{\alpha,k} \right\| e^{\frac{2\pi|k|}{2\tau}r} \nu^\alpha. \tag{28}$$

Also note that if f is a polynomial then, since $\mathbb{P}_{N,K}$ is a trigonometric polynomial, the expression given by (28) reduces to a finite sum. (If f is a non-polynomial analytic vector field then the expression is a finite sum plus a Taylor remainder).

Remark 2.19. • The utility of equation (28) in applications is that it gives us a well defined and easy to compute indicator which aids in choosing the numerical domain of approximation. We typically have in mind some fixed value of ϵ as a computational tolerance, and then determine reasonable values of N, K, ν, and $r > 0$ by numerical experimentation.
• Another advantage of using the Wiener-norm framework discussed here is that it sets the stage for the rigorous numerical computations to be taken up in the next paper in this series. We will see that while the choices of function spaces and norms made here are motivated by the desire for efficient numerics, these choices also provide exactly the right theoretical framework for computer assisted validation of the truncation error associated with the approximation of $\mathbb{P}$ by $\mathbb{P}_{N,K}$.
• The practical implication of the choice of $\nu > 0$ is easy to see, as this determines the "size" of the image of $\mathbb{P}_{N,K}$ in phase space. Taking larger values of ν corresponds to parameterizing larger local manifolds. We note that the value of $r > 0$ has somewhat more subtle, but still quite practical implication: it determines the width of the complex strip into which the parameterization can be extended analytically in the time variable. Since analytic bounds on the supremum norm of a function on a complex strip can be traded in for analytic bounds on the derivatives of the function on any smaller strip (via the classical Cauchy

bounds), larger values of r correspond to having more control of derivatives with respect to θ. Another way to think of this is that r controls the decay rates of the Fourier coefficients, that is larger values of r correspond to better decay rates for the Fourier coefficients of the manifold. These issues will be essential in the applications to computer assisted proof of connecting orbits between periodic orbits which will be addressed in the second paper in the series.

• The most difficult part of computing $\epsilon(r, \nu)$ is the computation of the Fourier-Taylor expansion of $f \circ \mathbb{P}$. If f is polynomial then the composition may be computed via convolution/Cauchy products, and the fast Fourier transform. In cases where the vector field is composed of only elementary functions the computation can often be worked out efficiently using the tools of automatic differentiation.

3 Computation of invariant manifolds: some examples

3.1 A case study: a-posteriori error for Lorenz

We are now ready to provide the details for the computations illustrated in Figures 1 and 2. As mentioned in the captions, the figures illustrate local stable/unstable manifolds for a hyperbolic periodic orbit which lies inside the Lorenz attractor at the classical parameter values. Performance results for the stable manifold are given in Table 1, while those for the unstable are given in Table 2. Recall that Figures 1 and 2 show the same manifolds from different angles with the stable in red and the unstable in blue. Both manifolds are local, in the sense that no integration has been applied in order to globalize the manifolds. All computations were done on a MacBook Pro, Intel Core 2 Duo, 2.33 GHz.

N	ν	r	$\epsilon = \epsilon(\nu, r)$	Computation Time	Error Computation Time
2	0.1	0.05	4.39×10^{-6}	0.47 sec	0.008 sec
2	0.1	0.01	7.96×10^{-10}	0.47 sec	0.008 sec
4	0.5	0.01	7.96×10^{-10}	0.82 sec	0.012 sec
10	6	0.01	8.19×10^{-10}	1.83 sec	0.029 sec
20	15	10^{-3}	6.47×10^{-9}	3.57 sec	0.071 sec
25	20	10^{-6}	1.77×10^{-6}	4.42 sec	0.096 sec

Table 1: Stable manifold data. For each computation, the periodic orbit, the Floquet normal form, and all manifold Taylor coefficients $a_n(\theta)$ are computed with $K = 66$ Fourier modes.

N	ν	r	$\epsilon(\nu, r)$	Computation Time	Error Computation Time
2	0.1	0.05	4.39×10^{-6}	0.47 sec	0.007 sec
2	0.1	0.01	7.96×10^{-10}	0.47 sec	0.008 sec
4	0.5	0.01	7.96×10^{-10}	0.82 sec	0.012 sec
10	6	0.01	8.67×10^{-10}	1.84 sec	0.03 sec
20	10	10^{-3}	6.12×10^{-9}	3.53 sec	0.071 sec
25	12	10^{-6}	2.39×10^{-7}	4.37 sec	0.097 sec

Table 2: Unstable manifold data. Again the periodic orbit, the Floquet normal form, and all manifold Taylor coefficients $a_n(\theta)$ are computed with $K = 66$ Fourier modes.

Both tables list the Taylor order N, the domain parameter $\nu > 0$ (which controls the extent of the local manifold in phase space), the size of the complex strip $r > 0$ used in the a-posteriori error error evaluation and the resulting a-posteriori error indicator ϵ. The

time taken to compute the parameterization coefficients (that is to solve the homological equations for up to order N) as well as the time required in order to evaluate the a-posteriori error are given. We note that the timings do not include the time required in order to compute the Fourier expansion of the orbit and its Floquet normal form.

For N large we can choose large parameter spaces (e.g. $\nu \in [6, 20]$ for the stable manifold). The manifolds shown in the figures correspond to those listed in the last lines of the tables, that is those computed to the highest order and having the largest parameter domains. These expansions were computed and verified in less than five seconds each.

For ν much larger than shown in the table the a-posteriori errors break down rapidly. Increasing the order does not lead to much improvement. We also note that, even in the case of the highest order expansions shown in these tables, the time devoted to evaluation of the a-posteriori error is virtually insignificant compared to the time needed to compute the coefficients. This confirms that once the parameterization is computed to a certain order it is not prohibitively expensive to compute optimal values for ν, r by "guess and check".

3.2 The Arneodo system

Consider the Arneodo system (with $\beta = 2$ and $\alpha = 3.372$)

$$\begin{cases} \dot{x} = y \\ \dot{y} = z \\ \dot{z} = \alpha x - x^2 - \beta y - z, \end{cases} \tag{29}$$

It admits a periodic orbit Γ with period roughly $\tau = 4.5328$. The complex matrix B in the complex Floquet normal form (4) has the following eigenvalues

$$\mu_1 = -1.0935 + 0.6931i, \qquad \mu_2 = 0.0935 + 0.6931i, \qquad \mu_3 = 0.$$

Since $\mathrm{Re}(\mu_1) < 0$ and $\mathrm{Re}(\mu_2) > 0$, $\dim(W^s(\Gamma)) = \dim(W^u(\Gamma)) = 1$. Two eigenvalues of B are of the form $\mu = \nu + \frac{i\pi}{\tau} \in \mathbb{C}$, as in second case of Remark 2.3. Each Floquet exponent corresponds to the Floquet multiplier $\phi_i = e^{\mu_i \tau}$, that is $\phi_1 = -0.0070$ and $\phi_2 = -1.5275$, which are both real negative. Hence, the orientation of the eigenvector $w_i(\theta) = Q(\theta)w_i$ is flipped over $[0, \tau]$ and the corresponding linear bundles are Mobius strips.

Remark 3.1. The local unstable manifold is plotted in figure 3 is the same manifold discussed in [24]. The difference between the pictures is in the methods used in order to obtain the local manifolds. Our figure 3 is the image of a Fourier-Taylor polynomial, while the image in [24] is obtained via a numerical globalization scheme applied to the linear approximation of the manifold.

In figure 4 we show a larger section of the local unstable manifold than is shown in [24] or in figure 3. Again the result illustrated in figure 4 emploies no numerical integration scheme. We have simply increased the number of Fourier and Taylor modes used in the computation.

This remark is in no way meant as a critique of the methods of [24]. Rather we aim to show that the results obtained using the Parameterization Method alone can in some cases reproduce results in the literature obtained via numerical integration. Again, this does not suggest that the Parameterization method is a replacement for numerical globalization schemes. Instead our hope is to highlight in the context of a specific example the point made in Remark 1.3: namely that combining the computational methods based on the Parameterization Method with globalization methods such as those discussed in [18] presents exciting possibilities for future research on invariant manifolds.

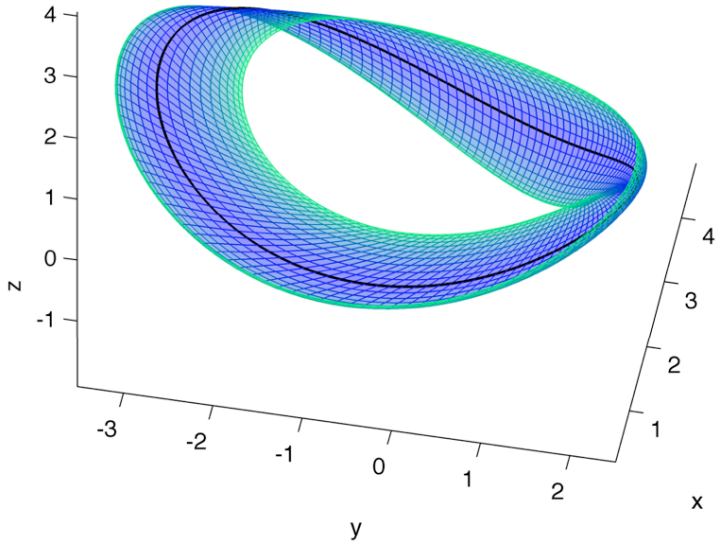

Figure 3: Unstable local manifold of the periodic orbit for the Arneodo system. In this figure the manifold is computed using 20 Fourier and 10 Taylor modes.

3.3 The Rössler system

We now compute a three dimensional stable manifold in the Rössler system

$$\begin{cases} \dot{x} = -(y+z) \\ \dot{y} = x + \frac{1}{5}y \\ \dot{z} = \frac{1}{5} + z(x-\lambda). \end{cases} \tag{30}$$

For small λ the system has a single fully attracting periodic orbit. As λ increases the periodic orbit undergoes a period doubling bifurcation giving rise to a chaotic attractor. We set $\lambda = 0.5$ and compute the periodic orbit and Floquet normal form using $K = 45$ Fourier modes. The period of the orbit is roughly $\tau = 5.0832$, the eigenvalues of B are real (and therefore coincide with the eigenvalues of R), and are given by $\lambda_1 = -0.16577$ and $\lambda_2 = -0.01044$. The orbit is stable and the corresponding Floquet multipliers are positive. Hence, the bundles are orientable. In this case computing the stable manifold of the orbit provides a trapping region for the orbit on which the dynamics are conjugate to linear. The stable manifold is illustrated in Figure 5.

3.4 The Kuramoto-Sivashinsky PDE

We conclude with a higher dimensional example which arises as a finite dimensional projection of a PDE. Consider the Kuramoto-Sivashinsky equation

$$\begin{aligned} &u_t = -u_{yy} - \lambda u_{yyyy} + 2uu_y \\ &u(t,y) = u(t,y+2\pi), u(t,-y) = -u(t,y), \end{aligned} \tag{31}$$

which is a popular model to analyze weak turbulence or *spatiotemporal chaos* [87, 88].

We expand solutions of (31) using Fourier series as

$$u(t,y) = \sum_{n\in\mathbb{Z}} c_n(t) e^{iny}. \tag{32}$$

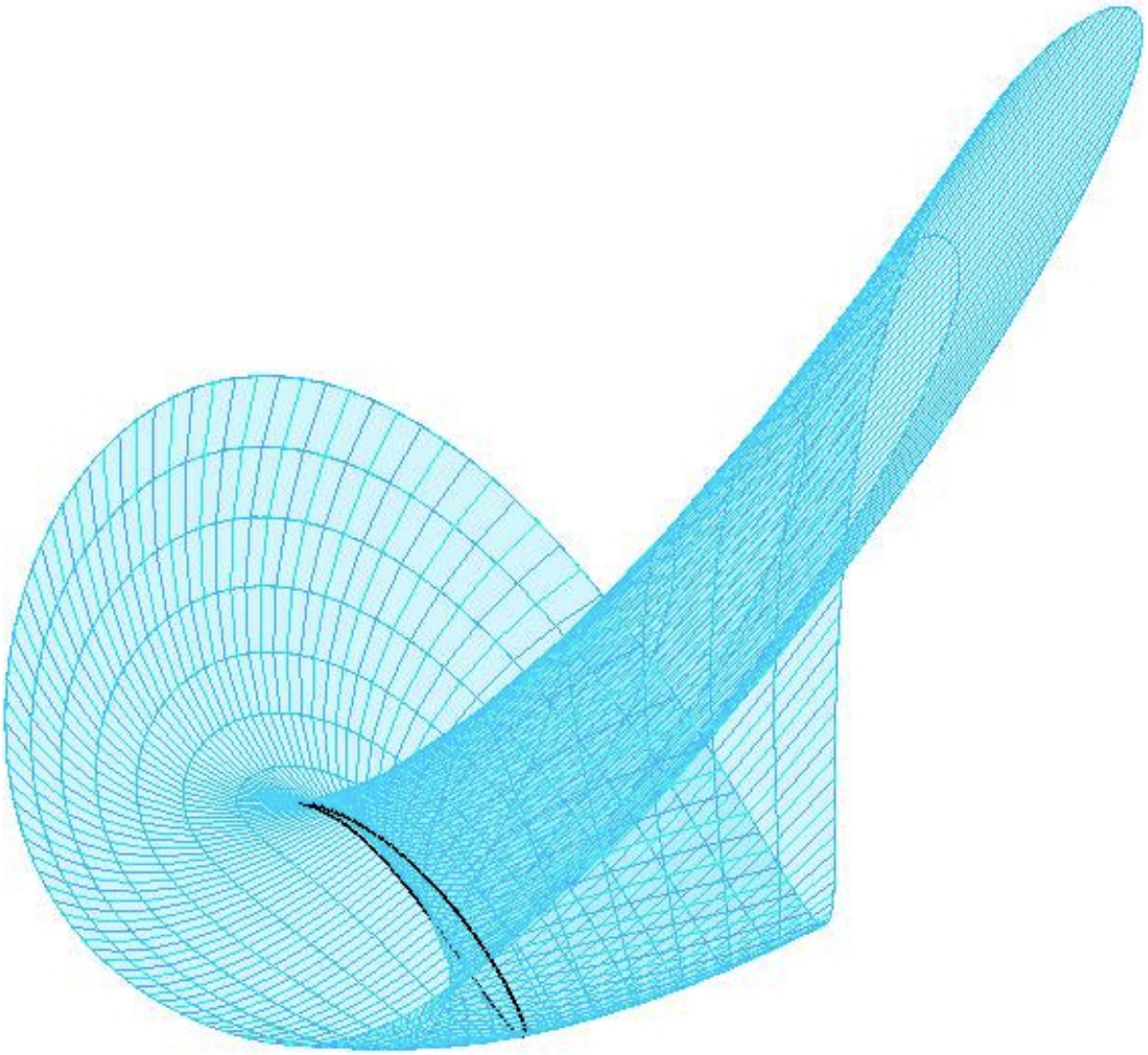

Figure 4: A "more global" depiction of the Arneodo manifold. This figure illustrates the same manifold shown in Figure 3 however in this case the local approximation is taken to 45 Fourier modes and 40 Taylor modes. We see more nonlinear features of the manifold, but it is more difficult to see the Mobius Strip. Carefully following the boundary curve shows that there is still only one component of the boundary.

The functions $\xi_n(t)$ so that $c_n(t) = i\xi_n(t)$ solve the infinite system of real ODEs

$$\dot{\xi}_n = (n^2 - \lambda n^4)\xi_n - n \sum_{n_1+n_2=n} \xi_{n_1}\xi_{n_2}, \tag{33}$$

where $\xi_{-n}(t) = -\xi_n(t)$, for all t, n. We consider a finite dimensional Galerkin projection of

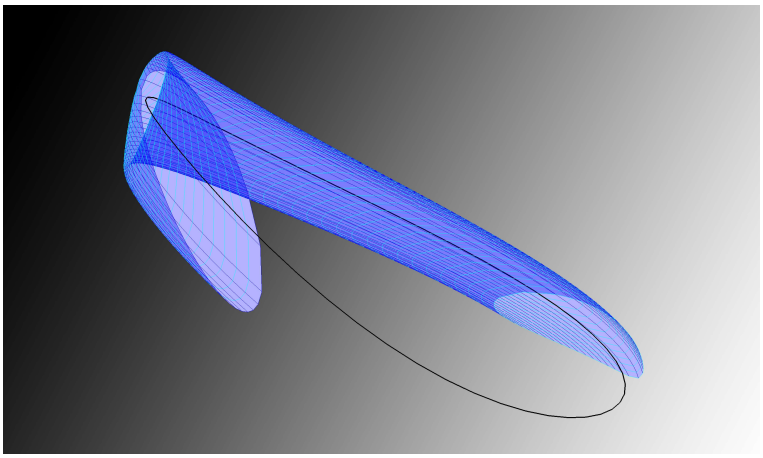

Figure 5: Boundary of a trapping region for the globally attracting periodic orbit of the Rössler system at $\lambda = 0.5$. The manifold is "cut away" to show the tubular quality of the trapping region. The trapping region is special in the sense that the dynamics in this tube is conjugate to the linear dynamics given by the linear flow (6). The conjugacy is given by the parameterization computed to Taylor order $N = 25$. The tube is the image of the Fourier-Taylor polynomial. No numerical integration is used to obtain this image.

(33) of dimension $m = 10$

$$\dot{\xi}_n = (n^2 - \lambda n^4)\xi_n - n \sum_{\substack{n_1+n_2=n \\ |k_i|\leq 10}} \xi_{n_1}\xi_{n_2}, \qquad (n = 1, \ldots, 10). \tag{34}$$

For $\lambda = 0.127$, we compute a periodic orbit Γ with period roughly $\tau = 2.2443$. We computed first a matrix B in the complex Floquet normal form (4) of $\Phi(t)$. The Floquet exponents (given by the eigenvalues B) are all real negative. In this case, the eigenvalues μ_i of B and λ_i of R coincide and are given by

	λ_1	λ_2	λ_3	λ_4	λ_5
10^3*	-1.1691	-0.7513	-0.4558	-0.2555	-0.1281
	λ_6	λ_7	λ_8	λ_9	λ_{10}
10^3*	-0.0535	-0.0147	-0.0021	-0.0006	0

Hence, the periodic orbit Γ is stable. All associated Floquet multipliers are real and by Remark 2.3, the associated eigenvector $w(\theta) = Q(\theta)w$ are not flipped over the interval $[0, \tau]$, and each associated bundle is orientable. Figure 6(a) shows the projection over the first three variables (ξ_1, ξ_2, ξ_3) of the local stable manifold associated to the eigenvalue $\lambda_9 = -0.5730$, that is the *slow* stable manifold of the periodic orbit. This illustrates the fact that the Parameterization Method allows computation of invariant sub-manifolds of the full stable manifold associated with *slow* eigendirections.

At $\lambda = 0.11878$ there is a solution with period $\tau = 3.894911$. The eigenvalues of B result to be real: one of them is positive that is $\lambda = 1.135682$, while the rest are negative. Hence there is one unstable direction. Figure 6(b) shows the local unstable manifold, again using the projection over the first three variables (ξ_1, ξ_2, ξ_3).

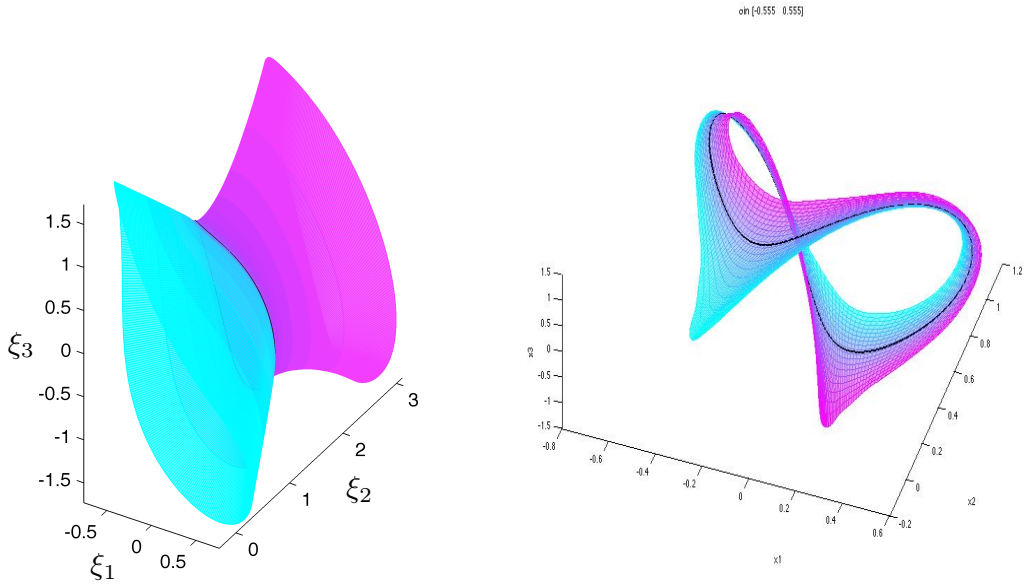

(a) (b)

Figure 6: (a) *Slow* local stable manifold of the periodic orbit at $\lambda = 0.127$. (b) Local unstable manifold of a periodic orbit at $\lambda = 0.11878$.

4 Preconditioning the method of projected boundary conditions using stable/unstable manifold parameterization and computation of connecting orbits

Local parameterizations of stable and unstable manifolds are useful for computing connecting orbits. The idea is to reformulate the connecting orbit as the solution of a finite time boundary value problem for an orbit segment beginning on the local unstable manifold and terminating on the local stable manifold. This idea goes back to [29] where it is used to compute connecting orbits between equilibria of differential equations. The idea is extended in [31, 32] in order to numerically compute point-to-cycle and cycle-to-cycle connecting orbits.

It is also shown in [30] that high order expansions for the (un)stable invariant manifolds can be used in order to stabilize the numerical computation of the connecting orbits. Other studies which utilize high order expansions of (un)stable manifolds in order to study connecting orbits between fixed points and equilibria of discrete time dynamical systems and differential equations are found in [55, 56]. This idea can also be exploited in order to obtain computer assisted proof of the existence of connecting orbits [59, 62, 60]. In this section we discuss some numerical computations for homoclinic connections of periodic orbits exploiting the high order parameterization of the present work.

Let $\Gamma_0 = \{\gamma_0(t) : t \in [0, \tau_0]\}$ and $\Gamma_1 = \{\gamma_1(t) : t \in [0, \tau_1]\}$ be hyperbolic periodic orbits for $\dot{x} = f(x)$. Suppose that Γ_0 has $\lambda_1^u, \ldots, \lambda_{k_0}^u$ unstable eigenvalues, that Γ_1 has $\lambda_1^s, \ldots, \lambda_{k_1}^s$ stable eigenvalues, and that $k_0 + k_1 = n - 1$. Let $\mathbb{P}\colon [0, \tau_0] \times B_{\nu_u}^{k_0} \subset \mathbb{R}^{k_0+1} \to \mathbb{R}^d$ and $\mathbb{Q}\colon [0, \tau_1] \times B_{\nu_s}^{k_1} \subset \mathbb{R}^{k_1+1} \to \mathbb{R}^d$ parameterize the local unstable and stable manifolds, that

is

$$\text{image}(\mathbb{P}) = W^u_{\text{loc}}(\Gamma_0) \qquad \text{and} \qquad \text{image}(\mathbb{Q}) = W^s_{\text{loc}}(\Gamma_1).$$

Furthermore we assume that $\mathbb{Q}$ solves (11) and that $\mathbb{P}$ solves (11) for the vector field $-f$. Then $\mathbb{P}$ and $\mathbb{Q}$ conjugate the dynamics on the stable/unstable manifolds to the linear flows.

The orbit of the point $x_0 \in \mathbb{R}^d$ is *heteroclinic* from Γ_0 to Γ_1 if

$$\alpha(x_0) \stackrel{\text{def}}{=} \bigcap_{s\in\mathbb{R}} \overline{\{\varphi(x_0,t) : t < s\}} = \Gamma_0 \qquad \text{and} \qquad \omega(x_0) \stackrel{\text{def}}{=} \bigcap_{s\in\mathbb{R}} \overline{\{\varphi(x_0,t) : t > s\}} = \Gamma_1.$$

If $\Gamma_0 = \Gamma_1$ then the orbit of x_0 is *homoclinic* for Γ_0. Heteroclinic points are equivalent to intersections of stable and unstable manifolds. Note that $\dim(W^s(\Gamma_0)) = k_0 + 1$, $\dim(W^u(\Gamma_1)) = k_1 + 1$, and that $\dim(W^s(\Gamma_0)) + \dim(W^u(\Gamma_1)) = n + 1$, and we are in the setting where we can look for generic transverse intersections.

A sufficient condition for the orbit of the point $\mathbb{P}(\hat{\theta}_0, \hat{\sigma}_0) \in \mathbb{R}^d$ to be heteroclinic from Γ_0 to Γ_1 is that

$$\varphi\left[\mathbb{P}(\hat{\theta}_0, \hat{\sigma}_0), L\right] = \mathbb{Q}(\hat{\theta}_1, \hat{\sigma}_1).$$

Note that this expression has n-components, and $n + 2$ variables $\theta_0, \sigma_0, \theta_1, \sigma_1$, and L. In order to define map from $\mathbb{R}^d$ into itself we impose the constraint (or phase condition) that $\|\sigma_0\| = R_0 < \nu_u$ and $\|\sigma_1\| = R_1 < \nu_s$. In other words we restrict to the surface of a sphere in parameter space. In this setting, where we compute high order parameterizations of the stable/unstable manifolds, these constraints provide natural phase conditions.

In order to formalize this notion let $S_{0,1} \colon \mathbb{S}^{k_{0,1}-1} \to \mathbb{R}^{k_{0,1}}$ be parameterizations of the $k_{0,1}$-spheres of radii R_0, R_1. Then we define the function $F \colon \mathbb{R}^d \to \mathbb{R}^d$ by

$$F(\theta_0, \phi_0, L, \theta_1, \phi_1) = \varphi\left[\mathbb{P}(\theta_0, S_0(\phi_0)), L\right] - \mathbb{Q}(\theta_1, S_1(\phi_1)), \tag{35}$$

and look for solutions of $F(\theta_0, \phi_0, L, \theta_1, \phi_1) = 0$. Since the map is now from $\mathbb{R}^d$ to itself we compute solutions using a numerical Newton scheme.

Note that there a many variations on equation (35). For example of we fix a "time of flight" $L > 0$ then we only have to constrain one of the variables $\sigma_{0,1}$. Then we obtain heteroclinic connection by looking for zeros of the function $G \colon \mathbb{R}^d \to \mathbb{R}^d$ defined by

$$G(\theta_0, \phi_0, \theta_1, \sigma_1) = \varphi\left[\mathbb{P}(\theta_0, S_0(\phi_0)), L\right] - \mathbb{Q}(\theta_1, \sigma_1),$$

We also note that both F and G as defined above assume that the flow φ is explicitly known. In practice however φ is only approximated by numerical integration.

For the purpose of doing computer assisted proofs it is useful to reformulate the boundary value problem in "integrated" form. This exploits the explicit dependance on the vector field f. For example (35) can be rewritten as the nonlinear operator $F \colon C^0([0, L]) \times \mathbb{R}^d \to C^0([0, L]) \times \mathbb{R}^d$ given by

$$F[u(t), \theta_0, \phi_0, \theta_1, \phi_1] = \begin{pmatrix} \mathbb{P}(\theta_0, S_0(\phi_0)) + \displaystyle\int_0^t f(u(s))\, ds - u(t) \\ \mathbb{Q}(\theta_1, S_1(\phi_1)) - \mathbb{P}(\theta_0, S_0(\phi_0)) - \displaystyle\int_0^L f(u(s))\, ds \end{pmatrix}, \tag{36}$$

which is solved for the unknown function $u(t)$ and numbers $(\theta_0, \phi_0, \theta_1, \phi_1)$. The operator is conveniently discretized by representing $u(t)$ using splines [62, 60] or Chebychev series [61].

4.1 Numerical results for connecting orbits

First we consider the Lorenz system with parameter values $s = 10$, $\beta = 8/3$, and $\rho = 30$. For these parameters the system is chaotic. The system is a good place to look for connecting orbits between periodic orbits as hyperbolic periodic orbits are dense on the attractor. Moreover each such periodic orbit has infinitely many homoclinic orbits. We choose the periodic orbit discussed in the introduction. Two homoclinic orbits for this periodic orbit are illustrated in Figure 7. Here we parameterize the stable/unstable manifolds to Taylor order $N = 25$ and solve (35) using a Newton scheme.

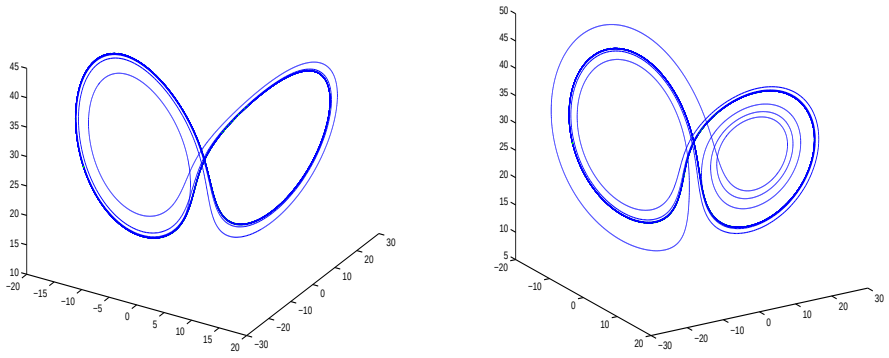

Figure 7: Two different orbits homoclinic to the same periodic orbit in the Lorenz system. The period of the orbit is roughly $\tau = 1.4860$. The "time of flight" for the orbit on the left is $L = 1.08145$ while for the orbit on the right we have $L = 3.50118$. The boundary conditions are projected onto manifolds of Taylor order $N = 15$ computed to $K = 45$ Fourier modes. The orbit illustrated on the left takes one "turn" around the left lobe of the Lorenz attractor after leaving the local unstable manifold and before returning to the local stable manifold. The orbit on the right on the other hand makes a "turn" on the left lobe of the attractor as well as a number of "turns" on the right lobe during its homoclinic excursion.

If we compute these orbits by projecting onto the linear approximation of the stable/unstable manifolds then the connecting orbits require about 35 time units in order to exhibit their full homoclinic behavior. In other words we see by numerical experimentation that 35 time units is approximately the amount of time required for a homoclinic orbit to start from a small neighborhood of the periodic orbit, make a homoclinic excursion, and return.

On the other hand when we precondition the projected boundary method via the parameterized stable/unstable manifolds the numerical integrations required when we solve the boundary value problem for the connecting orbits shown in Figure 7 are only $L \approx 1.1$ and $L \approx 3.5$ respectively. For the remainder of the time the orbits are on the local stable and unstable manifolds, as shown in Figure 8. Then computing these orbits using the linear approximation would require roughly 35 units of integration time, where as the present computations were carried out with less than four. In Figure 9, we show the time series for Lorenz homoclinics.

Figure 10 illustrates a similar computation performed for a hyperbolic periodic orbit of (31). Here we have taken a parameter value of approximately $\lambda = 0.119$, and the periodic

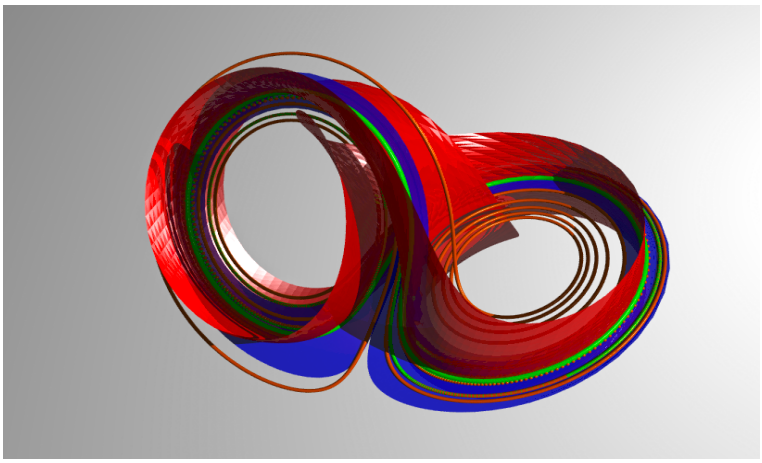

Figure 8: This figure illustrates the two homoclinic orbits shown in Figure 7, but here both orbits are shown in the same picture along with the local stable (red) and unstable (blue) manifolds onto which the boundary conditions are projected. The information about the number of modes used in the computation and the time of flights of the homoclinic orbits is given in the caption of the previous figure.

orbit has period roughly 1.95. This orbit has one unstable direction. The unstable manifold is parameterized using the methods of Section 3. The time of flight for the approximate connecting orbit shown in the Figure is $L = 14.5$ time units.

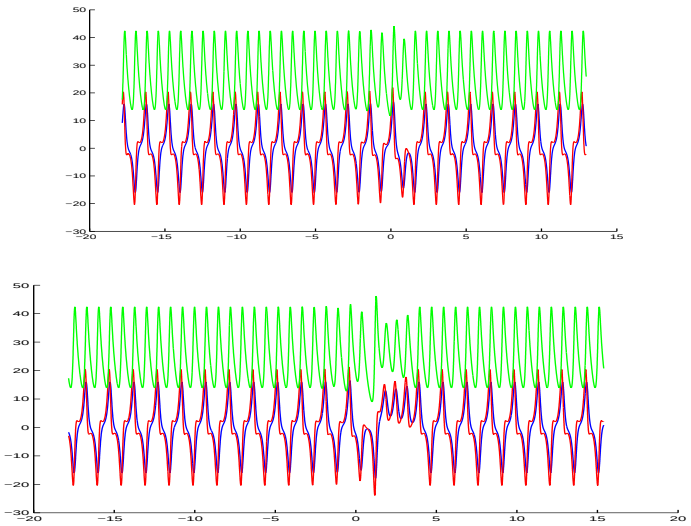

Figure 9: The figure illustrates the time series representation of the same homoclinic orbits shown in Figure 8. On the left and right hand sides of both the top and bottom orbit the behavior is indistinguishable from periodic. In the middle of both series we see a "wobble" away from the periodic orbit which signifies the homoclinic excursion.

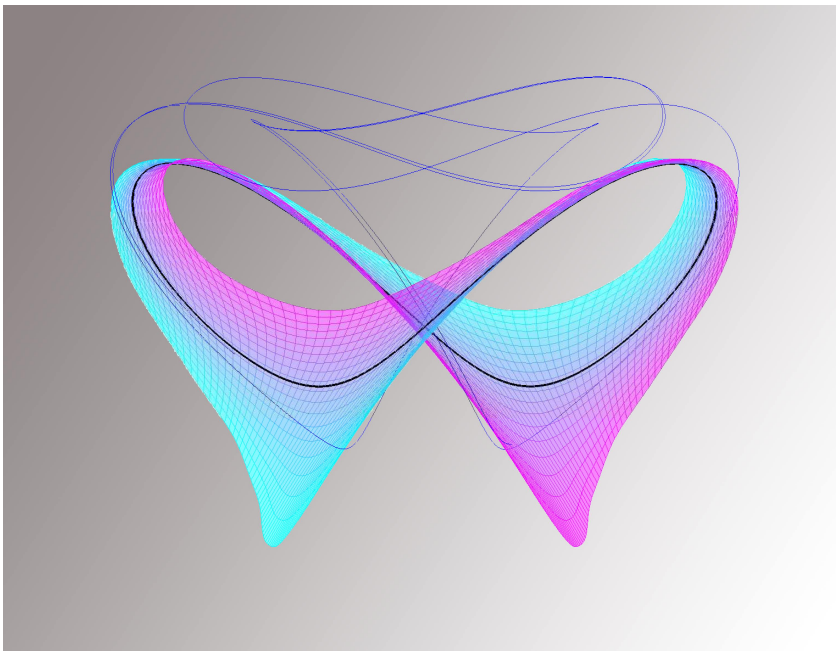

Figure 10: A homoclinic orbit in the 10-dimensional Galerkin projection of the Kuramoto-Sivashinsky PDE (34). The periodic orbit has one unstable direction and eight stable directions. We project the boundary conditions onto a high order Fourier-Taylor approximation of the unstable manifold, and onto the linear approximation of the stable manifold provided by the real Floquet normal form.

5 Acknowledgments

The authors would like to thank Rafael de la Llave for several illuminating discussions. The first author was partially supported by the MICINN grant MTM2011-24766. The third author was partially supported by NSF grant DSM 1318172.

References

[1] Marcio Gameiro and Jean-Philippe Lessard. Analytic estimates and rigorous continuation for equilibria of higher-dimensional PDEs. *J. Differential Equations*, 249(9):2237–2268, 2010.

[2] K.E. Davis, R.L. Anderson, D.J. Scheeres, Daniel and G.H. Born. The use of invariant manifolds for transfers between unstable periodic orbits of different energies, *Celestial Mech. Dynam. Astronom.*, Vol. 107, No. 4, 471–485, 2010.

[3] Kathryn E. Davis, Rodney L. Anderson, Daniel J. Scheeres, and George H. Born. Optimal transfers between unstable periodic orbits using invariant manifolds. *Celestial Mech. Dynam. Astronom.*, Vol. 109, No. 3, 241-264, 2011.

[4] D. Blazevski, D. and C. Ocampo. Periodic orbits in the concentric circular restricted four-body problem and their invariant manifolds, *Phys. D*, Vol. 241, No. 13, 1158–1167, 2012.

[5] F. Gabern, A. Jorba, and U. Locatelli. On the construction of the Kolmogorov normal form for the Trojan asteroids, *Nonlinearity*, Vol. 18, No. 4, 1705–1734, 2005.

[6] G. Gómez, J. Llibre, and J.J. Masdemont. Homoclinic and heteroclinic solutions in the restricted three-body problem, *Celestial Mech.*, Vol. 44, No. 3, 239–259, 1988/89.

[7] J. Llibre, R. Martínez, and C. Simó. Tranversality of the invariant manifolds associated to the Lyapunov family of periodic orbits near L_2 in the restricted three-body problem, *J. Differential Equations*, Vol. 58, No. 1, 104–156, 1985.

[8] W. S. Koon, M.W. Lo, J.E. Marsden, and S.D. Ross. Low energy transfer to the moon. *Celestial Mech. Dynam. Astronom.*, Vol. 81, No. 1-2, 63-73, 2000.

[9] G. Gómez, W. S. Koon, M. W. Lo, J. E. Marsden, J. Masdemont, and S. D. Ross. Connecting orbits and invariant manifolds in the spatial restricted three-body problem. *Nonlinearity*, Vol. 17, No. 5, 1571-1606, 2004.

[10] R. Castelli, Regions of prevalence in the coupled restricted three-body problems approximation. *Communications in Nonlinear Science and Numerical Simulation*, Vol. 17, No. 2, 804-816, 2012.

[11] A. Zanzottera, G. Mingotti, R. Castelli, M. Dellnitz, Intersecting invariant manifolds in spatial restricted three-body problems: Design and optimization of Earth-to-halo transfers in the Sun–Earth–Moon scenario. *Communications in Nonlinear Science and Numerical Simulation*, Vol. 17, No. 2, 832-843, 2012.

[12] W. S. Koon, M. W. Lo, J. E. Marsden, and S. D. Ross. Heteroclinic connections between periodic orbits and resonance transitions in celestial mechanics. *Chaos*, Vol. 10, No. 2, 427-469, 2000.

[13] C. Chicone, and W. Liu. Asymptotic phase revisited, *J. Differential Equations*, Vol. 204, No. 1, 227–246, 2004.

[14] C. Chicone, *Ordinary differential equations with applications*, Texts in Applied Mathematics, Vol. 34, 2nd ed., Springer, New York, 2006.

[15] J. Guckenheimer. Isochrons and phaseless sets, *J. Math. Biol.*, Vol. 1, No. 3, 259–273, 1974/75.

[16] F. Gabern, W.S. Koon, S. Wang, J.E. Marsden, and S.D. Ross. Theory and computation of non-RRKM lifetime distributions and rates in chemical systems with three or more degrees of freedom, *Phys. D*, Vol. 211, No. 3-4, 391–406, 2005.

[17] F. Lekien, C. Coulliette, A.J. Mariano, E.H. Ryan, L.K. Shay, G. Haller, and J.E. Marsden. Pollution release tied to invariant manifolds: a case study for the coast of Florida, *Phys. D*, Vol. 210, No. 1-2, 1–20, 2005.

[18] B. Krauskopf, H. M. Osinga, E. J. Doedel, M. E. Henderson, J. Guckenheimer, A. Vladimirsky, M. Dellnitz, and O. Junge. A survey of methods for computing (un)stable manifolds of vector fields. *Internat. J. Bifur. Chaos Appl. Sci. Engrg.*, Vol. 15, No. 3, 763-791, 2005.

[19] J. Guckenheimer and A. Vladimirsky. A fast method for approximating invariant manifolds, *SIAM J. Appl. Dyn. Syst.*, Vol. 3, No. 3, 232–260, 2004.

[20] T. Sahai, and A. Vladimirsky. Numerical methods for approximating invariant manifolds of delayed systems, *SIAM J. Appl. Dyn. Syst.*, Vol. 8, No. 3, 1116–1135, 2009.

[21] M. Dellnitz, and A. Hohmann, Andreas. A subdivision algorithm for the computation of unstable manifolds and global attractors, *Numer. Math.*, Vol. 75, No. 3, 293–317, 1997.

[22] B. Krauskopf, H.M. Osinga. Computing geodesic level sets on global (un)stable manifolds of vector fields, *SIAM J. Appl. Dyn. Syst.*, Vol. 2, No. 4, 546–569, 2003.

[23] B. Krauskopf, and H. Osinga. Two-dimensional global manifolds of vector fields, *Chaos*, Vol. 9, No. 3, 1054–1500, 1999.

[24] H.M. Osinga. Nonorientable manifolds in threee-dimensional vector fields, *Internat. J. Bifur. Chaos Appl. Sci. Engrg.*, Vol. 13, No. 3, 553–570, 2003.

[25] M.E. Johnson, M.S. Jolly, and I.G. Kevrekidis, Ioannis Two-dimensional invariant manifolds and global bifurcations: some approximation and visualization studies, *Numer. Algorithms*, Vol. 14, No. 1-3, 125–140, 1997.

[26] P. Aguirre, E.J. Doedel, B. Krauskopf, H.M. Osinga. Investigating the consequences of global bifurcations for two-dimensional invariant manifolds of vector fields, *Discrete Contin. Dyn. Syst.*, Vol. 29, No. 4, 1309–1344, 2011.

[27] E.J. Doedel, B. Krauskopf, and H.M Osinga. Global invariant manifolds in the transition to preturbulence in the Lorenz system, *Indag. Math. (N.S.)*, Vol. 22, No. 3-4, 222–240, 2011.

[28] Àngel Jorba, and Jordi Villanueva. Numerical computation of normal forms around some periodic orbits of the restricted three-body problem. *Phys. D*, Vol. 114, No. 3-4, 197-229, 1998.

[29] E.J. Doedel, and M.J. Friedman. Numerical computation of heteroclinic orbits, Continuation techniques and bifurcation problems, *J. Comput. Appl. Math.*, Vol 26, No. 1-2, 15–170, 1989.

[30] M.J. Friedman, and E.J. Doedel. Computational methods for global analysis of homoclinic and heteroclinic orbits: a case study. *J. Dynam. Differential Equations*, Vol. 5, No. 1, 37–57, (1993).

[31] E. J. Doedel, B. W. Kooi, G. A. K. van Voorn, and Yu. A. Kuznetsov. Continuation of connecting orbits in 3D-ODEs. I. Point-to-cycle connections. *Internat. J. Bifur. Chaos Appl. Sci. Engrg.* Vol. 18, No. 7, 1889-1903, 2008.

[32] E. J. Doedel, B. W. Kooi, G. A. K. Van Voorn, and Yu. A. Kuznetsov. Continuation of connecting orbits in 3D-ODEs. II. Cycle-to-cycle connections. *Internat. J. Bifur. Chaos Appl. Sci. Engrg.* Vol. 19, No. 1, 159-169, 2009.

[33] R.C. Calleja, E.J. Doedel, A.R. Humphries, A. Lemus-Rodríguez, and E.B. Oldeman. Boundary-value problem formulations for computing invariant manifolds and connecting orbits in the circular restricted three body problem, *Celestial Mech. Dynam. Astronom.*, Vol. 114, No. 1-2, 77–106, 2012.

[34] E. Canalias, and J.J. Masdemont. Homoclinic and heteroclinic transfer trajectories between planar Lyapunov orbits in the sun-earth and earth-moon systems, *Discrete Contin. Dyn. Syst.*, Vol. 14, No. 2, 261–279, 2006.

[35] L. Arona, and J.J. Masdemont. Computation of heteroclinic orbits between normally hyperbolic invariant 3-spheres foliated by 2-dimensional invariant tori in Hill's problem, *Discrete Contin. Dyn. Syst.*, Dynamical Systems and Differential Equations. Proceedings of the 6th AIMS International Conference, suppl. 64–74, 2007.

[36] E.M. Alessi, G. Gómez, and J.J. Masdemont. Leaving the Moon by means of invariant manifolds of libration point orbits, *Commun. Nonlinear Sci. Numer. Simul.*, Vol. 14, No. 12, 4153–4167, 2009.

[37] C. Simó. On the Analytical and Numerical Approximation of Invariant Manifolds. *Les Méthodes Modernes de la Mecánique Céleste* (Course given at Goutelas, France, 1989), 285-329, Editions Frontiéres, Paris, 1990.

[38] A. Jorba, and J.J. Masdemont. Dynamics in the center manifold of the collinear points of the restricted three body problem, *Physica D. Nonlinear Phenomena*, Vol. 132, No. 1-2, 189–213, 1999.

[39] A. Jorba, and J. Villanueva. Numerical computation of normal forms around some periodic orbits of the restricted three-body problem, *Phys. D*, Vol. 114, No. 3-4, 197–229, 1998.

[40] E. Belbruno, M. Gidea, and F. Topputo. Weak stability boundary and invariant manifolds, *SIAM J. Appl. Dyn. Syst.*, Vol. 9, No. 3, 1061–1089, 2010.

[41] E. Belbruno, M. Gidea, and F. Topputo. Geometry of weak stability boundaries. *Qualitative Theory of Dynamical Systems*, Vol. 12, 53-66, 2013.

[42] J.K. Wróbel, and R.H. Goodman, High-order adaptive method for computing two-dimensional invariant manifolds of three-dimensional maps, Commun. Nonlinear Sci. Numer. Simul., Vol. 18, No. 7, 1734–1745, 2013.

[43] R. H. Goodman, and J. K. Wróbel, High-order bisection method for computing invariant manifolds of two-dimensional maps, Internat. J. Bifur. Chaos Appl. Sci. Engrg., Vol. 21, No. 7, 2017–2042, 2011.

[44] W.J. Beyn. The numerical computation of connecting orbits in dynamical systems. *IMA Journal of Numerical Analysis*, vol. 10 (1990), no. 3, 379-405.

[45] X. Cabré, E. Fontich, and R. de la Llave. The Parameterization Method for Invariant Manifolds. I. Manifolds Associated to Non-resonant Subspaces. *Indiana Univ. Math. J.*, 52(2):283-328, (2003).

[46] X. Cabré, E. Fontich, and R. de la Llave. The Parameterization Method for Invariant Manifolds. II. Regularity with Respect to Parameters. *Indiana Univ. Math. J.*, 52(2):329-360, (2003).

[47] X. Cabré, E. Fontich, and R. de la Llave. The parameterization method for invariant manifolds. III. Overview and applications. *J. Differential Equations*, 218(2):444–515, 2005.

[48] D. Viswanath, Divakar, The Lindstedt-Poincaré technique as an algorithm for computing periodic orbits, *SIAM Rev.*, Vol. 43, No. 3, 478–495, 2001.

[49] J.E. Doedel, M.J. Friedman, and A.C. Monteiro, On locating connecting orbits, *Appl. Math. Comput.* vol 65, (1994), no 1-3, 231-239.

[50] B. Krauskopf, and T. Rieß, A Lin's method approach to finding and continuing heteroclinic connections involving periodic orbits. *Nonlinearity*, vol. 21 (2008), no. 8, 1655-1690.

[51] J. Knobloch, and T. Rieß, Lin's method for heteroclinic chains involving periodic orbits, *Nonlinearity*, vol. 23 (2010), no. 1, 23-54.

[52] S. Smale. Diffeomorphisms with Many Periodic Points. 1965 Differential and Combinatorial Topology (A Symposium in Honor of Marston Morse) pp. 63-80 *Princeton Univ. Press*, Princeton, N.J.

[53] D. Wilczak. Abundancs of Heteroclinic and Homoclinic Orbits for the Hyperchaotic Rössler System. *Discrete Contin. Dyn. Syst. Ser. B 11* (2009), no. 4, 1039-1055.

[54] D. Wilczak, and P. Zgliczyński, Heteroclinic connections between periodic orbits in planar restricted circular three body problem. II *Communications in Mathematical Physics*, vol. 259 (2005), no. 3, 561-576.

[55] J.D. Mireles James, and Hector Lomelí. Computation of Heteroclinic Arcs with Application to the Volume Preserving Hénon Family. *SIAM J. Applied Dynamical Systems*, Volume 9, Issue 3, pp 919-953, 2010.

[56] J.D. Mireles James Quadratic Volume-Preserving Maps: (Un)stable Manifolds, Hyperbolic Dynamics, and Vortex Bubble Bifurcations. *Journal of Nonlinear Science*, Volume 23, Number 4, 2013, pp. 585–615.

[57] R. de la Llave, and J.D. Mireles James. Parameterization of Invariant Manifolds by Reducibility for Volume Preserving and Symplectic Maps. *Discrete and Continuous Dynamical Systems.* Volume 32, Number 12, December 2012. pp 4321–4360.

[58] G. Moore, Floquet theory as a computational tool, *SIAM J. Numer. Anal.*, Vol 42., 2522–2568, 2005.

[59] J.D. Mireles James, and K. Mischaikow, Rigorous a posteriori computation of (un)stable manifolds and connecting orbits for analytic maps, SIAM J. Appl. Dyn. Syst., Vol, 12, No. 2, 957–1006, 2013.

[60] J.P. Lessard, J.D. Mireles James, and C. Reindardt, Computer Assisted Proof of Transverse Saddle-to-Saddle Connecting Orbits for First Order Vector Fields. (Submitted).

[61] J.P. Lessard, and C. Reinhardt. Rigorous numerics for nonlinear differential equations using Chebyshev series. *SIAM Journal on Numerical Analysis*, Vol. 52, No. 1, 1–22, (2014).

[62] J.B. van den Berg, J.D. Mireles-James, J.P Lessard, and K. Mischaikow, Rigorous numerics for symmetric connecting orbits: even homoclinics of the Gray-Scott equation, SIAM J. Math. Anal., Vol. 43, No. 4, 1557–1594, 2011.

[63] J.P. Boyd, *Chebyshev and Fourier Spectral Methods*, 2nd ed., Dover Publications, Inc., New York, 2000.

[64] R. de la Llave. A tutorial on KAM theory, Smooth ergodic theory and its applications (Seattle, WA, 1999), *Proc. Sympos. Pure Math.*, Vol 69, pp. 175-292, 2001.

[65] R. de la Llave, A. González, A. Jorba, and J. Villanueva. KAM theory without action-angle variables, *Nonlinearity*, 18(2) pp. 855-895, (2005).

[66] Á. Haro, and R. de la Llave. A Parameterization Method for the Computation of Invariant Tori and Their Whiskers in Quasi-Periodic Maps: Numerical Algorithms. *Discrete Contin. Dyn. Syst. Ser. B* 6 (2006), no. 6, 1261-1300.

[67] Á. Haro, and R. de la Llave. A Parameterization Method for the Computation of Invariant Tori and their Whiskers in Quasi-Periodic Maps: Rigorous Results. *J. Differential Equations* 288 (2006), no. 2, 530-579.

[68] M. Canadell, and A. Haro. Parameterization method for computing quasi-periodic reducible normally hyperbolic invariant tori, Proceedings CEDYA 2013.

[69] M. Canadell, and A. Haro. A Newton-like method for computing normally hyperbolic invariant tori, *Chapter 5 of Computation of Invariant Manifolds with parametrization methods*, (In progress).

[70] E. Freire, A. Gasull, and A. Guillamon. Limit cycles and Lie symmetries, *Bull. Sci. Math.*, Vol. 131, No. 6, 501–517, 2007.

[71] A. Guillamon and G. Huguet. A Computational and Geometric Approach to Phase Resetting Curves and Surfaces. *SIAM Journal on Applied Dynamical Systems*, Vol 8, Issue 3, pp. 1005-1042 (2009).

[72] G. Huguet and R. de la Llave. Computation of limit cycles and their isochrons: fast algorithms and their convergence, *SIAM J. Appl. Dyn. Syst.*, 12(4), 1763–1802, 2013.

[73] E. Fontich, R. de la Llave, and Y. Sire. A Method for the Study of Whiskered Quasi-Periodic and Almost-Periodic Solutoins in Finite and Infinite Dimensional Hamiltonian Systems. *Electronic Research Announcements in Mathematical Sciences* Vol 16, pp. 9-22, (2009).

[74] R. Calleja, and R. de la Llave. Fast Numerical Computation of Quasi-Periodic Equilibrium States in 1D Statistical Mechanics, Including Twist Maps. *Nonlinearity* 22 (2009), no. 6, 1311-1336.

[75] R. Calleja, and R. de la Llave. A Numerically Accessible Criterion for the Breakdown of Quasi-Periodic Solutions and its Rigorous Justification. *Nonlinearity* 23 (2010), no. 9, 2029-2058.

[76] R.C. Calleja, Renato, A. Celletti, and R. de la Llave. A KAM theory for conformally symplectic systems: efficient algorithms and their validation, *J. Differential Equations*, Vol. 255, No. 5, 978–1049, 2013.

[77] W. Tucker, Robust normal forms for saddles of analytic vector fields, Nonlinearity, Vol. 17, No. 5, 1965–1983, 2004.

[78] T. Johnson, and W. Tucker, Warwick, A note on the convergence of parametrised non-resonant invariant manifolds, Qual. Theory Dyn. Syst., Vol. 10, No. 1, 107–121, 2011.

[79] W. Tucker, The Lorenz attractor exists, C. R. Acad. Sci. Paris Sér. I Math., Vol. 328, No. 12, 1197–1202, 1999.

[80] R. Castelli, J.-P. Lessard. Rigorous numerics in Floquet theory: computing stable and unstable bundles of periodic orbits. *SIAM J. Appl. Dyn. Syst.* 12 (2013), no. 1, 204245.

[81] R. Castelli, J.-P. Lessard. A method to rigorously enclose eigenpairs of complex interval matrices. *Proceedings of the International Conference on Applications of Mathematics (AM2013)* in honour of the 70-th birthday of Karel Segeth, Institute of Mathematics AS CR, Prague 2013.

[82] A. M. Fox, and J.D. Meiss. Efficient Computation of Invariant Tori in Volume-Preserving Maps. *Submitted.*

[83] T. Blass, and R. de la Llave. KAM theory for volume-preserving maps. *Submitted.*

[84] E. Canalias, A. Delshams, J.J. Masdemont, and P Roldán. The scattering map in the planar restricted three body problem. *Celestial Mech. Dynam. Astronom.* Vol. 95, No. 1-4, 155-171, (2006).

[85] A. Delshams, J.J Masdemont, and P. Roldán. Computing the scattering map in the spatial Hill's problem. *Discrete Contin. Dyn. Syst. Ser. B* Vol. 10, No. 2-3, 455–483, (2008)

[86] M.J. Capiński, and P. Roldán. Existence of a center manifold in a practical domain around L_1 in the restricted three-body problem. *SIAM J. Appl. Dyn. Syst.* Vol. 11, No. 1, 285–318, (2012)

[87] Y. Kuramoto and T. Tsuzuki. Persistent propagation of concentration waves in dissipative media far from thermal equilibrium. *Prog. Theor. Phys.*, 55(365), 1976.

[88] G. I. Sivashinsky. Nonlinear analysis of hydrodynamic instability in laminar flames. I. Derivation of basic equations. *Acta Astronaut.*, 4(11-12):1177–1206, 1977.